

LA-10545-MS

UC-34

Issued: October 1985

Electromagnetic Signals from Underground Nuclear Explosions

John Malik
Robert Fitzhugh
Fred Homuth

Reproduced From
Best Available Copy



DISTRIBUTION STATEMENT A
Approved for Public Release
Distribution Unlimited

20000907 120

Los Alamos Los Alamos National Laboratory
Los Alamos, New Mexico 87545

DTIC QUALITY INSPECTED 4

A9400-08-1889

CONTENTS

ABSTRACT.....	1
I. INTRODUCTION.....	1
II. DIPOLE MODELS.....	5
III. SEISMOELECTRIC MODEL.....	14
IV. CONCLUSIONS.....	19
APPENDIX A. EARTH POTENTIAL, MAGNETIC FIELD, AND CABLE CURRENT DATA FROM A LOW-YIELD EVENT (D--) IN ALLUVIUM.....	21
APPENDIX B. USEFUL LAPLACE TRANSFORMS AND MODIFIED BESSEL FUNCTION RELATIONS.....	31
I. LAPLACE TRANSFORMS.....	31
II. ASYMPTOTIC EXPANSIONS OF MODIFIED BESSEL FUNCTION RELATIONS FOR LARGE X.....	32
APPENDIX C. SCALING RELATIONS FOR UNDERGROUND NUCLEAR EXPLOSIONS.....	33
APPENDIX D. GEOLOGIC SETTING FOR EVENT LOWBALL.....	35
APPENDIX E. EARTH MOTION DATA OBTAINED BY R. FITZHUGH FROM EVENT LOWBAL...	39
APPENDIX F. DATA OBTAINED BY F. HOMUTH ON UNDERGROUND EVENTS.....	41
APPENDIX G. FITZHUGH'S LOWBALL DATA.....	49
REFERENCES.....	61
OTHER USEFUL SOURCES.....	61

FIGURES

Fig. 1.	Record of the horizontal electric field components for the Bilby event at 7.62 km south (magnetic) of the shot point.....	2
Fig. 2.	Radial and azimuthal fields from a low-yield event emplaced in alluvium.....	3
Fig. 3.	Radial and azimuthal fields from an intermediate-yield event emplaced in rhyolite.....	4
Fig. 4.	Radial electric fields from a delta-function horizontal electric dipole at 30- and 0-m depth.....	9
Fig. 5.	Radial electric field from a delta-function horizontal electric dipole at 715-m depth. The late shoulder is the slow pulse of Fig. 4; the larger amplitude is due to propagation to the surface, thence along the surface to the detector at 6.7 km. The slow pulse is propagated through the medium on a direct path.....	10
Fig. 6.	Graphs of $F(x) = (1/2 - 1/x) x^{-5/2} e^{-1/x}$ and $\int_0^x F(u) du$ as functions of x	13
Fig. 7.	Geologic influence on EMP signals.....	16
Fig. 8.	Yucca fault.....	18
Fig. A-1.	Station layout for the low-yield event D--.....	23
Fig. A-2.	Typical differential circuits for earth-current measurements....	24
Fig. A-3.	Data from west location: upper, N-S plates; lower, E-W plates.....	25
Fig. A-4.	Data from east location: upper, N-S plates; lower, E-W plates.....	26
Fig. A-5.	Potential data from south location: upper, N-S plates; lower, E-W plates.....	27
Fig. A-6.	Radial magnetic field from south location.....	28
Fig. A-7.	Azimuthal magnetic field from south location.....	29
Fig. A-8.	Current on single signal cable.....	30
Fig. A-9.	Current on ground bus.....	30

Fig. C-1.	Radii vs time for a 1-kt explosion at 675 m in alluvium. Scaled from 10- and 300-kt calculations by T. Cook of Los Alamos. Initial conditions: energy in 1-m-radius iron gas sphere of mass 6 Mg.....	34
Fig. D-1.	E-W geologic cross section through U7av.....	37
Fig. D-2.	N-S geologic cross section through U7av.....	38
Fig. E-1.	Earth motion data. Acceleration in g's vs t and velocity in m/s vs t at 15 m from ground zero.....	40
Fig. F-1.	Lowball Event EMP--Buried plates across Yucca fault.....	42
Fig. F-2.	Draughts Event EMP--Buried plates near seep.....	43
Fig. F-3.	Rummy Event EMP--Plates in drill hole UelK.....	44
Fig. F-4.	Draughts Event EMP--Plates in drill hole UelK.....	45
Fig. F-5.	Draughts Event EMP--Buried plates across Yucca fault.....	46
Fig. F-6.	Draughts Event EMP--Buried plates near U9cn.....	47
Fig. G-1.	Locations of ground potential plates used on Lowball.....	50
Fig. G-2.	Data from GM-1 plates - 1.37 km, NW.....	51
Fig. G-3.	Data from GM-4 plates - 1.04 km, W.....	52
Fig. G-4.	Data from GM-6 plates - 1.48 km, N.....	53
Fig. G-5.	Data from GM-8 plates - 2.01 km, WNW.....	54
Fig. G-6.	Data from GM-9 plates - 2.20 km, NNW.....	55
Fig. G-7.	Differential between GM-6 and GM-8 plates E/W, 2.05-km separation--3- and 30-ms time bases.....	56
Fig. G-8.	Differential between GM-6 and GM-8 (upper) and GM-4 and GM-9 (lower)--6-s time bases.....	57
Fig. G-9.	Potential on trailer park ground--30-ms time bases.....	58

TABLES

TABLE A-I. SUMMARY OF DATA FROM THE LOW-YIELD EVENT D--.....	22
TABLE D-I. PHYSICAL PROPERTY SUMMARY.....	36
TABLE G-I. DISTANCE TO POTENTIAL PLATES.....	49
TABLE G-II. LOWBALL SUMMARY.....	60

ELECTROMAGNETIC SIGNALS FROM UNDERGROUND NUCLEAR EXPLOSIONS

by

John Malik, Robert Fitzhugh, and Fred Homuth

ABSTRACT

Electromagnetic fields and ground currents resulting from underground nuclear explosions have been observed since the first such event. A few measurements have been reported, but most have not. There also have been some speculations as to their origin; the two most generally proposed are the magnetic bubble and the seismoelectric effect. The evidence seems to favor the latter mechanism.

I. INTRODUCTION

Electromagnetic fields and ground currents resulting from underground nuclear explosions have been observed from the earliest such explosion (1958). Despite over two decades of sporadic investigations, the data are fragmentary and either incompletely or unconvincingly interpreted. Some qualitative postulates of some mechanisms for generation of the signals¹ were suggested in March 1964.*

Using above-ground electric field probes, loops, and current transformers on cables with recording bandwidths exceeding 30 MHz, investigators at Sandia confirmed the existence of short-duration signals of low amplitudes (<1 V/m at 1 km), which emanated from impedance discontinuities (equalizers, recording shelters, cable splices, etc.) rather than from the well head. Among the best late-time data are those of Zablocki,² Fitzhugh,³ and Homuth. These data generally are differential measurements of the voltage between shallowly buried electrodes. Zablocki used a spacing of 750 m; Fitzhugh, 61

*This report is a combination of two memos written in 1980--one assuming the source to be due to electric or magnetic dipoles, the other considering the source to be seismoelectric in character. Then as now there was no definite conclusion, although the seismoelectric mechanism seems more likely. The memos received limited distribution and received no comment.

122 m; and Homuth used about 150 m. Zablocki's Bilby data are reproduced in Fig. 1; he also quotes a scaling law

$$(|E| = 2.2 \cdot 10^2 W^{0.44} / R^3 \text{ } \mu\text{V/m}) \text{ ,}$$

with W in kilotons and R in kilometers, resulting from measurements on several events. Examples of Fitzhugh's data are shown in Fig. 2 for the case of a low-yield event buried in alluvium and in Fig. 3 for a high-yield event (Inlet) buried in rhyolite. (See Appendix A.)

Both Bilby and Inlet were fired in cased holes; the hole for the low-yield event was uncased. Both had canister/rack support cables of wire rope from a strong-back at the surface and a number of coaxial and multiconductor cables from the downhole device canister/rack to the surface. These slow, low amplitude fields appear to propagate by diffusion through the earth, not by the less dispersive path of to the surface, thence along the surface to the electrodes. If the source could be approximated by elementary dipoles, either electric or magnetic, both modes ought to be observable with comparable integrals over time.

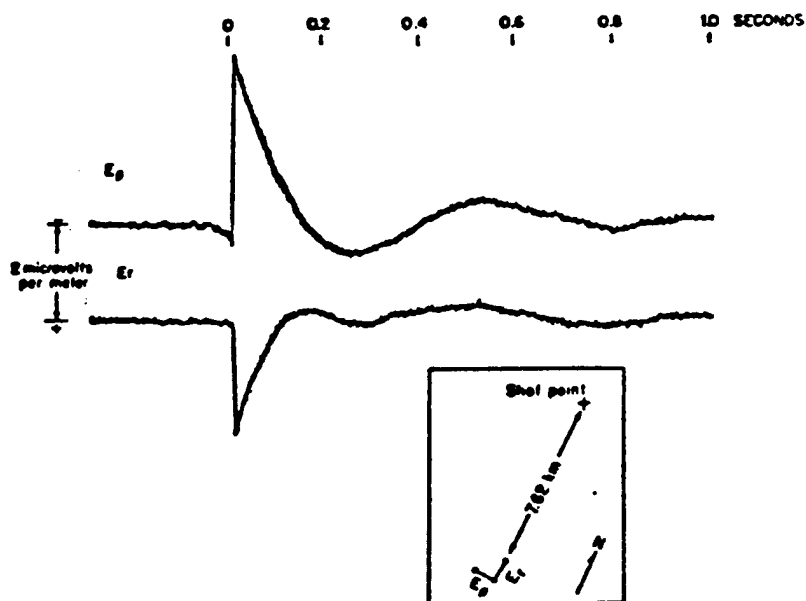


Fig. 1. Record of the horizontal electric field components for the Bilby event at 7.62 km south (magnetic) of the shot point.

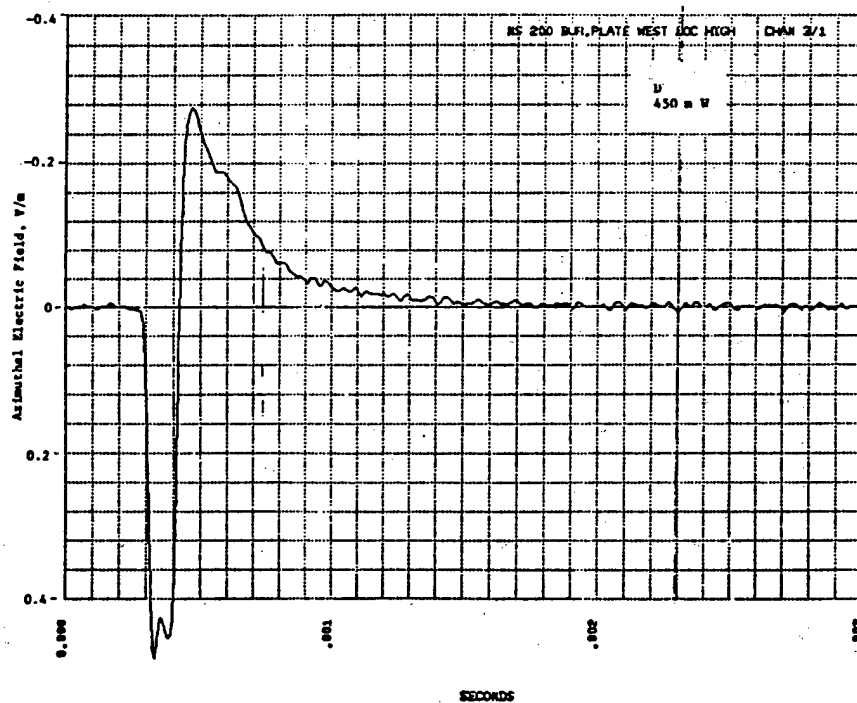
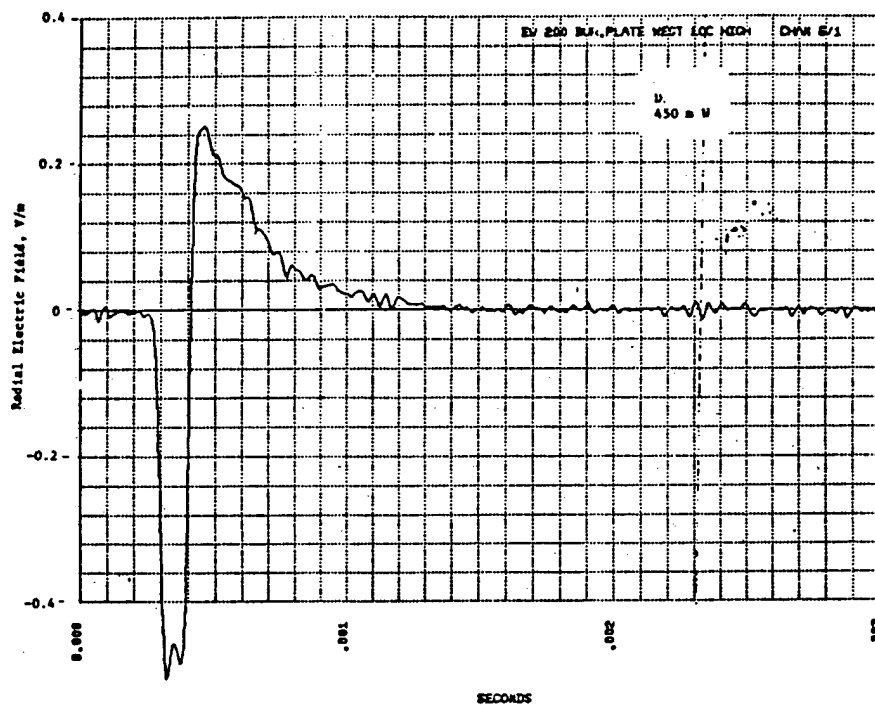


Fig. 2. Radial and azimuthal fields from a low-yield event emplaced in alluvium.

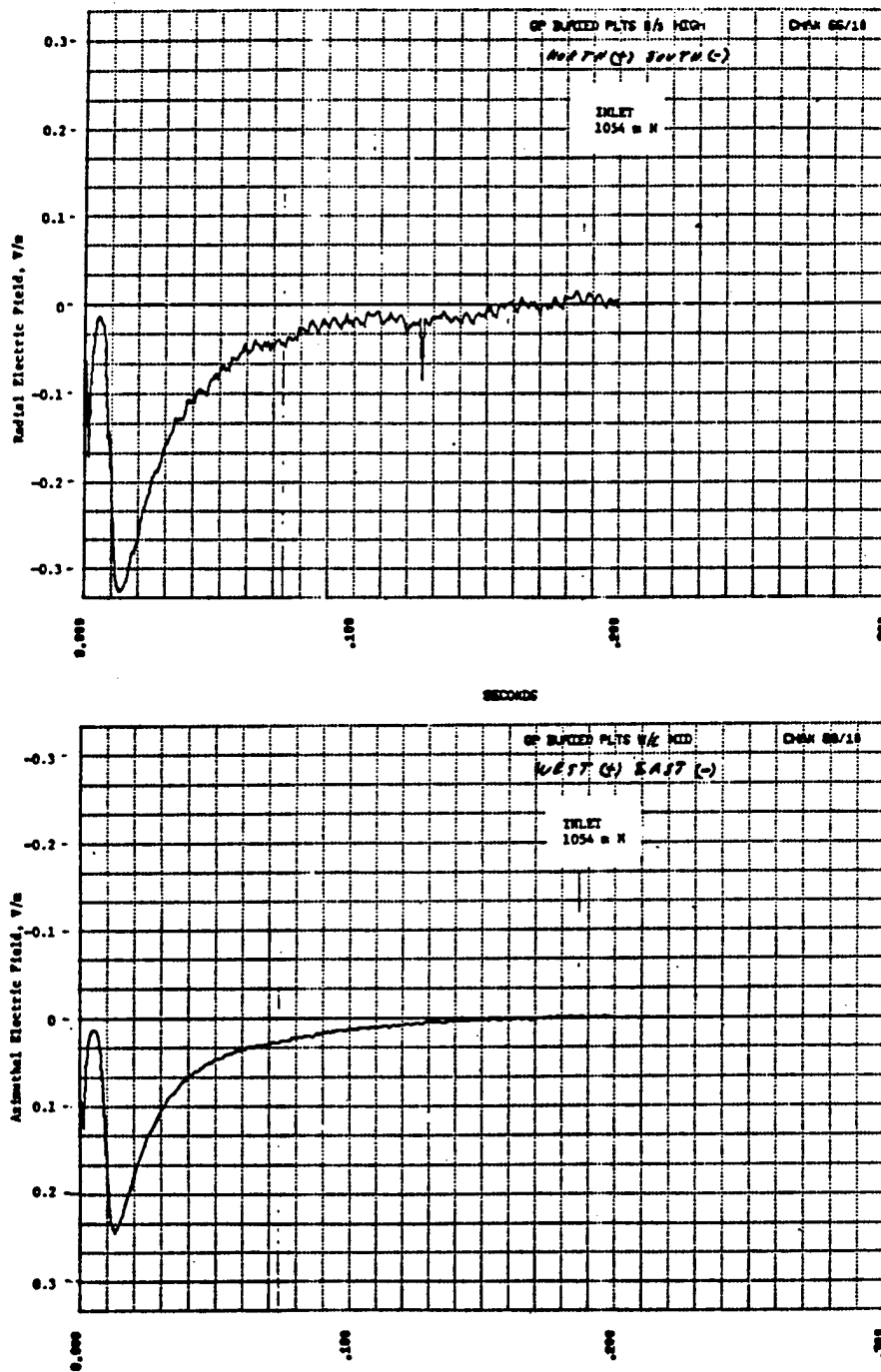


Fig. 3. Radial and azimuthal fields from an intermediate-yield event emplaced in rhyolite.

II. DIPOLE MODELS

Assuming the signals are due to electrical or magnetic effects, the theoretical base for understanding the signals was formulated in 1908 by A. Sommerfeld⁴ with substantial contributions from B. van der Pol and K. A. Norton. Basically, the simplified problem is specifying the source moment and solving Maxwell's equation in a two-medium geometry. The Navy (for underwater communications) and the mining industry (for location of ore deposits) have supported considerable investigations. The most notable investigators are A. Banos⁵ (University of California at Los Angeles), R. K. Moore and W. E. Blair⁶ (University of New Mexico), and J. R. Wait (National Bureau of Standards).⁷ The excellent treatise by Banos gives the field description from electric and magnetic dipoles on or in a conduction half-space; the summary relations are incomplete (as are those of Moore and Blair) and contain only the best propagation path (to the surface, thence along the surface to the observer). Other investigators that should be noted are C. N. Vittitoe (Sandia Laboratory) and L. Miller (Los Alamos National Laboratory), who calculated the above-ground fields from an underground horizontal magnetic dipole.⁸

Formulation of the integral equations, even with the guidance of the works of Sommerfeld and van der Pol, has been inconsistent and fraught with incompleteness and error. The works of Wait and Banos are very useful. In particular, Banos⁵ shows that the horizontal electric dipole is the best radiator, with the horizontal magnetic dipole as second best. Both are enormously better than vertical dipoles; the electric dipoles are better radiators than the magnetic ones. Banos also shows that the character of the fields is the same for the horizontal electric and magnetic dipole except for the replacement of the azimuthal dependence ϕ by $\phi + \pi/2$, and replacement of the electric dipole moment $p = I dl$ by $-imk$, where m is the magnetic moment and $k = (i\omega\mu\sigma)^{1/2}$.

One of the more informative developments of the fields from a horizontal δ -function electric dipole on the surface or at a depth h in a conducting medium (adaptable to a horizontal magnetic dipole) is by J. R. Wait (1960).⁷

For an observer on the surface [$z = 0$, but $h \neq 0$], Wait's Eqs. (101), (102), and (103) reduce to:

$$e_x(t) = \frac{4I}{\pi\sigma} \left\{ -\frac{h}{Tt} \left[\frac{I_1 - I_0}{2T} + \left(\frac{y}{T}\right)^2 (I_1' - 2I_1 + I_0) \right] \exp\left(-\frac{\rho^2}{T} - \frac{2h^2}{T}\right) - \left[2\left(\frac{h}{T}\right)^2 - \frac{1}{2T} \right] p(r,t) \right\} ,$$

$$e_y(t) = \frac{4I}{\pi\sigma} \left\{ \frac{xyh}{T^3 t} (I_1' - 2I_1 + I_0) \exp\left(-\frac{\rho^2}{T} - \frac{2h^2}{T}\right) \right\} ,$$

and

$$e_z = 0 .$$

The argument of the Bessel functions, I_0 , I_1 , I_1' , is $\rho^2/T = (x^2 + y^2) \mu\sigma/8t$ and $T = 8t/\mu\sigma$. It is useful to use the asymptotic expansion of the functions for large argument. (Comparison of numerical evaluations of the asymptotic expansions with the exact values gives indistinguishable results, <1% error for the situations of interest.) (See Appendix B.)

$$I_0(\zeta) - I_1(\zeta) \approx \frac{e^\zeta}{2\zeta\sqrt{2\pi\zeta}}$$

and

$$I_1'(\zeta) - 2I_1(\zeta) + I_0(\zeta) = 2I_0 - \left(2 + \frac{1}{\zeta}\right)I_1 \approx \frac{3e^\zeta}{4\zeta^2\sqrt{2\pi\zeta}} .$$

The first term in the braces of e_x becomes

$$\frac{\sqrt{\mu\sigma} h}{16\sqrt{\pi} \rho^3 t^{3/2}} \left[1 + \frac{3y^2}{\rho^2} \right] \exp\left(-\frac{\mu\sigma h^2}{4t}\right) .$$

The characteristic time is $\mu\sigma h^2/4$. This term corresponds to propagation to the surface, then along the surface with negligible further loss to the observer.

The second term in the braces of e_x becomes

$$\left[\frac{1}{2T} - 2 \frac{h}{T} \right] \sqrt{\frac{2}{\pi}} \frac{8}{\mu \sigma T^{3/2}} \exp\left(-2 \frac{r^2}{T}\right)$$

or

$$\frac{1}{4r^3} \left(\frac{1}{2} - \frac{\mu \sigma h^2}{4t} \right) \left[\frac{2 \cdot 4}{\sqrt{\pi} \mu \sigma r^2} \left(\frac{\mu \sigma r^2}{4t} \right)^{5/2} \exp\left(-\frac{\mu \sigma r^2}{4t}\right) \right] .$$

Setting $h = 0$, this is just one-half the expression for propagation from a dipole in an infinite medium, and it is thus the term for propagation through the medium along the direct path from source to observer.

The asymptotic expansion for e_y shows that the only propagation path is the up-and-over one.

The asymptotic relations are

$$\begin{aligned} e_x(t) &\approx \frac{4I}{\pi \sigma} \frac{d1}{8\rho^3} \left\{ \left(1 + \frac{3y^2}{\rho^2} \right) \left[\frac{4}{\sqrt{\pi} \mu \sigma h^2} \left(\frac{\mu \sigma h^2}{4t} \right)^{3/2} \exp\left(-\frac{\mu \sigma h^2}{4t}\right) \right] \right. \\ &\quad \left. + \frac{1}{4r^3} \left(\frac{1}{2} - \frac{\mu \sigma h^2}{4t} \right) \left[\frac{2 \cdot 4}{\sqrt{\pi} \mu \sigma r^2} \left(\frac{\mu \sigma r^2}{4t} \right)^{5/2} \exp\left(-\frac{\mu \sigma r^2}{4t}\right) \right] \right\} , \\ e_y(t) &\approx \frac{4I}{\pi \sigma} \frac{d1}{8\rho^5} \left\{ \frac{3xy}{\sqrt{\pi} \mu \sigma h^2} \left(\frac{\mu \sigma h^2}{4t} \right)^{3/2} \exp\left(-\frac{\mu \sigma h^2}{4t}\right) \right\} \end{aligned}$$

$$e_z = 0 ,$$

with

$$\rho^2 = x^2 + y^2$$

and

$$r^2 = \rho^2 + h^2 .$$

The expressions are written for easier interpretation; the integrals over time of all the square-bracket terms are unity, and the diffusion times are given by $\tau = \mu\sigma r^2/4$ or $\mu\sigma h^2/4$, depending on the propagation path. For a source on the surface ($h = 0$), the terms involving τ_h reduce to delta functions.

One way a horizontal electric dipole signal could be created is through an excitation of the horizontal cable runs or a downhole asymmetry in Compton and return currents (hard to conceive). The function $(\tau/t)^{n/2} e^{-\tau/t}$ has a maximum at $t = 2\tau/n$, and its integral over time is $\tau \Gamma(n/2 - 1)$.

For the cases of interest here,

<u>n</u>	<u>t_{max}</u>	<u>f_{max}</u>	<u>Integral</u>
3	$2\tau/3$	0.410	$\tau\sqrt{\pi}$
5	$2\tau/5$	0.811	$\tau\sqrt{\pi}/2$
7	$2\tau/7$	2.422	$\tau \cdot 3\sqrt{\pi}/4$

For a source and/or a receiver below the interface, there are two components with comparable integrals over time: one is due to propagation through a distance ($z + h$); the other is due to propagation through an infinite medium as noted earlier. To demonstrate this separation, three cases were computed using the exact expressions for the Zablocki conditions (range = 6.7 km). With the source and receiver at the interface, the fast component (to this degree of approximation) would be a delta function; to spread out this component, the source was put at a 30-m depth, with the characteristic time as $\mu\sigma h^2/4 = 3 \mu\text{s}$. This is shown in Fig. 4. Note that the peak field is near the characteristic time; the late-time fields fall as $t^{-3/2}$. To show the slow time component, the source and receiver were located at the interface; the fast component--a delta function for these conditions--is omitted. The characteristic time here is related to the receiver distance; that is, 0.14 s. If the source were at the depth of burial of Bilby (715 m), the field dependence for both linear and logarithmic time scales would be as given in Fig. 5.

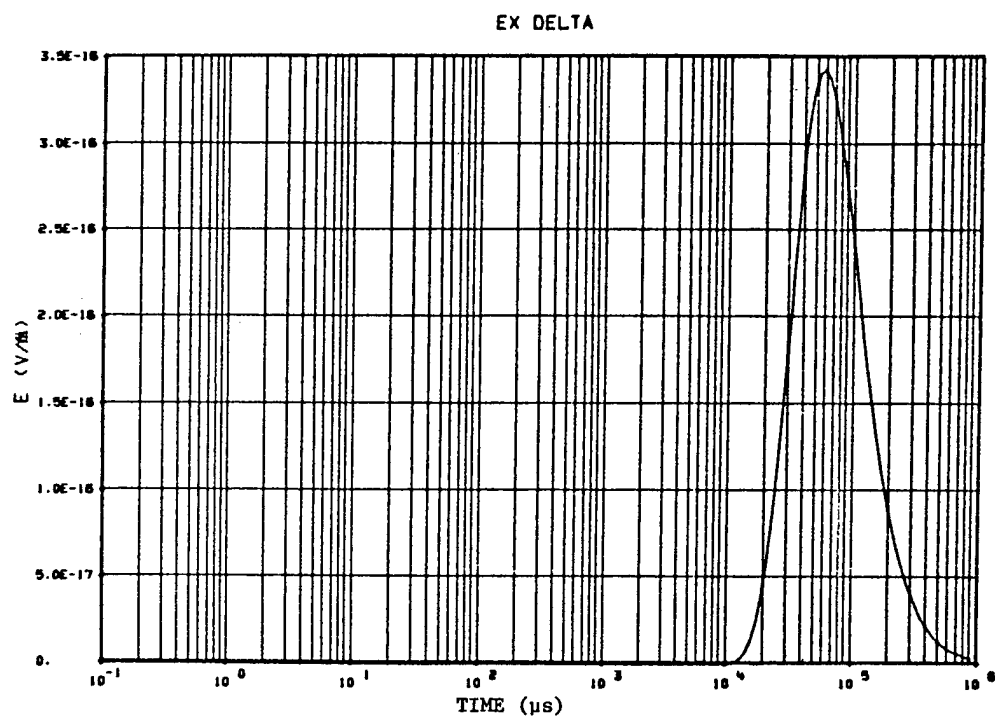
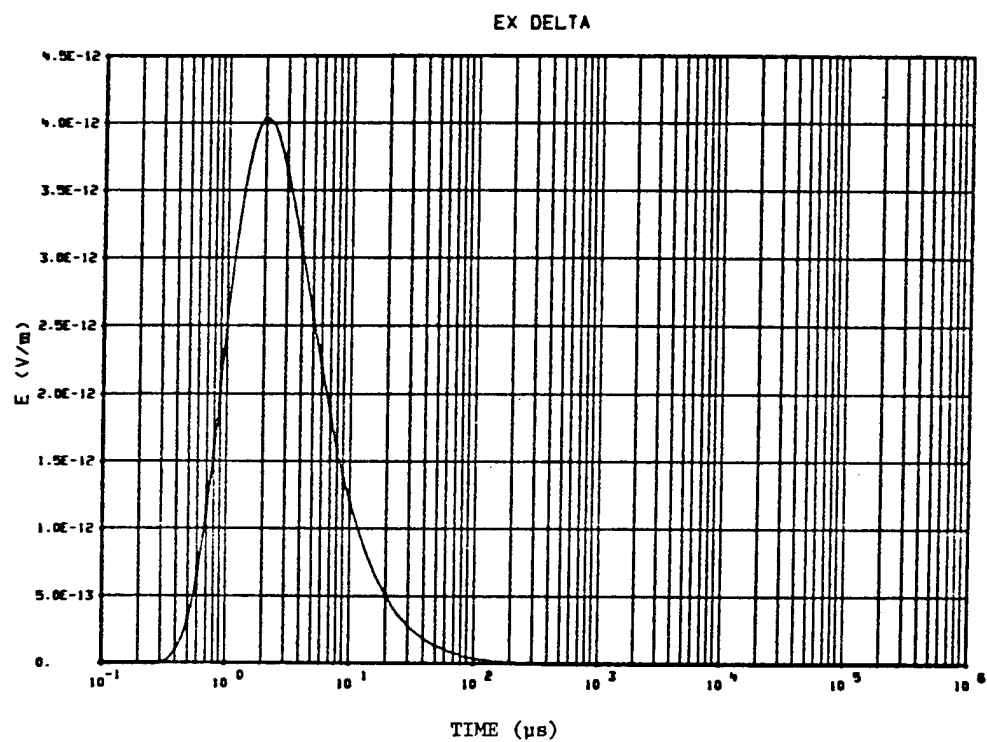


Fig. 4. Radial electric fields from a delta-function horizontal electric dipole at 30- and 0-m depth.

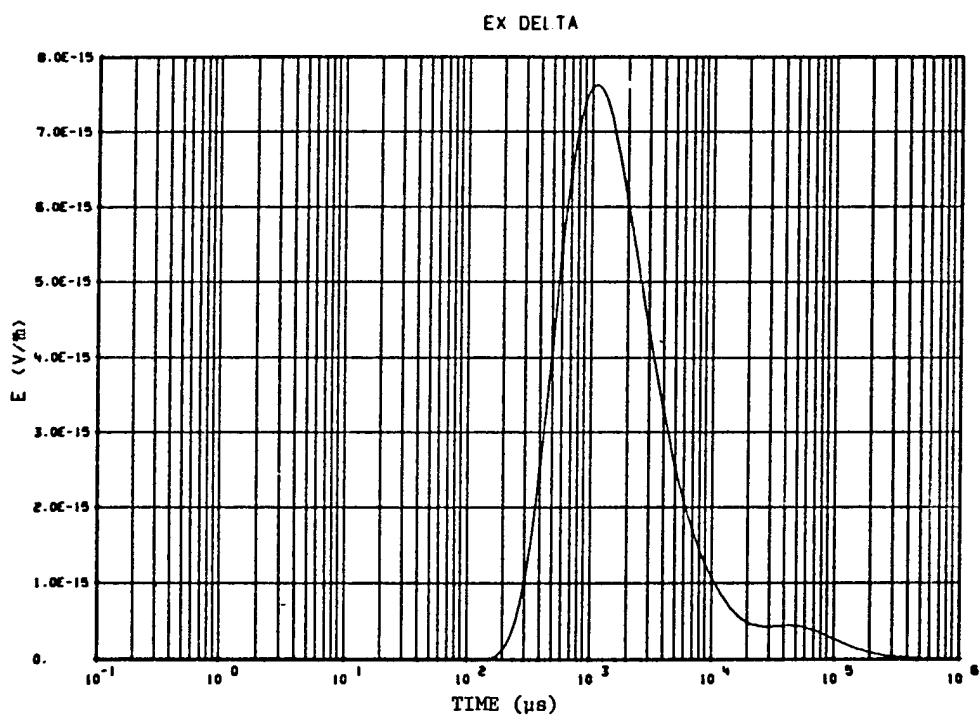
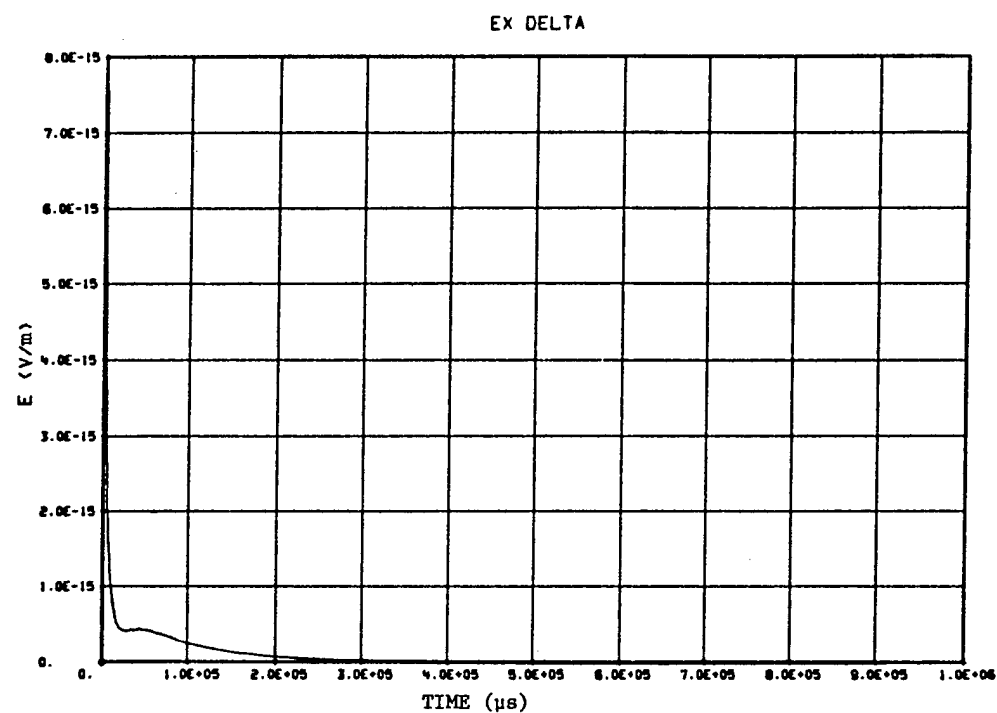


Fig. 5. Radial electric field from a delta-function horizontal electric dipole at 715-m depth. The late shoulder is the slow pulse of Fig. 4; the larger amplitude is due to propagation to the surface, thence along the surface to the detector at 6.7 km. The slow pulse is propagated through the medium on a direct path.

The fields measured by Zablocki on Bilby ought to correspond to the e_x fields--i.e., oriented in direction along the cable runs--but the data do not really fit any of these dependences; the data also show an azimuthal component that ought to be zero. The duration fits closely what would be expected for propagation through the medium. The peak is at about 10 ms--too long for the fast component and too short for the long component. Nor does the shape agree--there is no reversal of the fields.

There is also interest in fields from a magnetic dipole, notably in evaluating the "magnetic bubble" model--that is, the expulsion of the static geomagnetic field by the fireball and cavity. As noted earlier, the fields from horizontal electric and magnetic dipoles are of the same character, but with ϕ replaced by $\phi + \pi/2$ and p by $-imk = -im\sqrt{i\omega\mu\sigma}$.

From Wait's Eqs. (96) and (97),⁷

$$P_o = L \{p(r_o, t) u(t)\}$$

and

$$P = L \{p(r, t) u(t)\} ,$$

and for Eq. (99)

$$p(r, t) = \left(\frac{2}{\pi}\right)^{1/2} \frac{8}{\mu\sigma T^{3/2}} \exp(-2 r^2/T) ,$$

$$T = 8t/\mu\sigma ,$$

$$P = \frac{\exp[-(\mu\sigma s)^{1/2} r]}{r} ,$$

$$\frac{dP}{dr} = -(\mu\sigma s)^{1/2} P - \frac{P}{r} ,$$

or

$$\begin{aligned}
 -(\mu\sigma s)^{1/2} P &= \frac{dP}{dr} + \frac{P}{r} \\
 &= L \left\{ \frac{dp(r,t)}{dr} u(t) \right\} + \frac{1}{r} L \{p(r,t) u(t)\} \\
 &= \left(-\frac{4r}{T} + \frac{1}{r} \right) L \{p(r,t) u(t)\} .
 \end{aligned}$$

This permits a formal solution for the fields propagated through the medium. In the asymptotic approximation, the long-term fields from a horizontal magnetic dipole of moment m located at a depth h below the interface are

$$\begin{aligned}
 e_x &= 0 , \\
 e_y &\approx \frac{2m}{\pi\sigma r^4} \left(\frac{1}{2} - \frac{\mu\sigma r^2}{4t} \right) \left(\frac{1}{2} - \frac{\mu\sigma h^2}{4t} \right) \left[\frac{2 \cdot 4}{\sqrt{\pi} \mu\sigma r^2} \left(\frac{\mu\sigma r^2}{4t} \right)^{5/2} \exp\left(-\frac{\mu\sigma r^2}{4t}\right) \right] ,
 \end{aligned}$$

and

$$e_z = 0 .$$

This is for a delta-function moment. For a step-function moment (u), the fields are

$$\begin{aligned}
 e_{xu} &= 0 , \\
 e_{yu} &\approx \int_0^t e_{y\delta} dt ,
 \end{aligned}$$

and

$$e_{zu} = 0 .$$

The zeroes come at $t = \mu\sigma r^2/2$ and $\mu\sigma h^2/2$. The relations are shown in Fig. 6 for $h = 0$. (For most cases the effect of the factor containing h is small.)

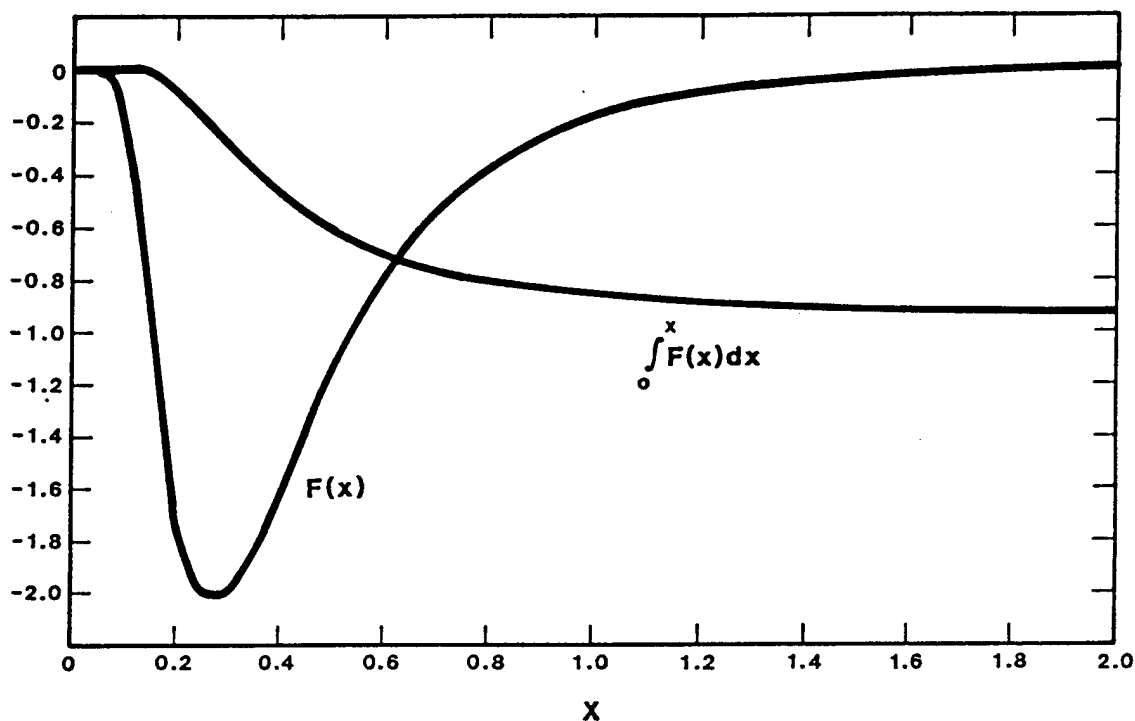


Fig. 6. Graphs of $F(x) = (1/2 - 1/x) x^{-5/2} e^{-1/x}$ and $\int_0^x F(u) du$ as functions of x .

The magnetic moment produced by the expulsion of a field B_0 from a sphere of radius R is

$$m = \frac{2\pi B_0 R^3}{\mu} .$$

For Bilby, the cavity radius was about 73 m. Taking the horizontal component of the geomagnetic field as $0.23 \cdot 10^{-4}$ tesla,

$$m \approx 4.5 \times 10^7 \text{ Am}^2 .$$

(Note that this assumes the conductivity of the melt and/or vapor is infinite.) The melt conductivity is probably in the range of a few siemens per meter; the vapor conductivity may be high and may remain so for some minutes. The thickness of the melt is a few tenths of a meter; hence, the

radius is very near that of the cavity. See Appendix C for cavity-radius and rate-of-growth scaling relations. It seems probable that the step-function relation is more appropriate; the time dependence, however, is not appropriate (Fig. 6).

However, taking the moment m as $4.5 \cdot 10^7 \text{ Am}^2$ [it was assumed as $m\delta(t)$], the peak field under all the assumptions including $\sigma = 10^{-2} \text{ S/m}$ is

$$e_y = \frac{2 \cdot 4.5 \cdot 10^7 \cdot 8 \cdot 2.08}{\pi^{3/2} \mu (10^{-2})^2 (7.6 \cdot 10^3)^6} \approx 11 \cdot 10^{-6} \text{ V/m} .$$

Zablocki observed $2.3 \cdot 10^{-6} \text{ V/m}$.

The amplitude and time dependence of the expected fields from the "magnetic bubble" make it a contender as the source of part of the observed fields under some assumptions that may not be viable. (The previous negative evaluation of these was based on use of formulae for vertical magnetic dipole.) The observed fields, however, do not exhibit the proper radial and azimuthal dependences. The time dependences are those due to propagation, and any electrical source would exhibit similar time scales. There are also later signals in the recorded data that cannot be explained by the "bubble." These, and perhaps part of the prompt signals, are discussed in Sec. III. It seems probable that the signals are due to more than one mechanism.

III. SEISMOELECTRIC MODEL

Slow, low amplitude fields that appear to diffuse through the earth have been observed by Zablocki,² Fitzhugh,³ Homuth, and others. Zablocki and Keller⁹ proposed that the source mechanism is the seismic-electric effect, though the evidence was not conclusive. They also measured similar signals on the Scooter event, an explosion of 500 tons of chemical explosives. Earlier, Martner and Sparks¹⁰ observed electrical signals from 1- to 20-lb HE charges detonated in bore holes. They attributed the signals to the electroseismic effect. Their results indicated that the signal amplitude is proportional to the square root of the charge weight. Extrapolating their data to the nuclear case, their relation for the electric fields in the earth near the epicenter gives the relations

$$E = 0.1 W^{0.5} \text{ V/m} ,$$

where the energy W is in kilotons. The amplitudes measured by Fitzhugh at ranges of 0.5 to 1.0 km are consistent with the relation (Appendix A).

The seismoelectric effect was first reported by Ivanov (1939), who alleged that the effect was due to electrofiltration phenomena in moist soil. Frenkel¹¹ presented a mathematical explanation based on the Helmholtz theory of filtration potentials: "The particles of moist soil are immersed in water which plays the role of the dispersive medium. The boundary surface between these particles and the water is the seat of electric double layers, whose aqueous side has a diffuse structure. The presence of such layers explains the connection between the flow of water in the capillary spaces of the soil and the transfer of the surface electrical charges gives rise to an electric field, in which case electrical currents are compensated by the volume conduction currents. According to the theory of Helmholtz and Smoluchovski, the difference of hydrostatic pressure Δp between two points of the soil must be connected with a difference of electrical potential

$$\Delta V = \frac{\epsilon \zeta}{4\pi\mu\sigma} \Delta p ,$$

where ζ is the electrokinetic potential, i.e., the potential drop in the surface double layer, μ the viscosity of water, and σ its electrical conductivity. Since the propagation of longitudinal elastic waves in the soil is accompanied by a variation of the pressure in the direction of propagation, it must also be accompanied by a variation of the electrical potential which constitutes the E-effect discovered by Ivanov.... In the case of Poiseuille flow in the liquid through a capillary tube with radius r , the average velocity of flow \bar{v} is connected with the pressure gradient by the relation

$$\bar{v} = - \frac{r^2}{8\mu} \frac{\partial p}{\partial x} . "$$

Substituting into the previous relation,

$$E = \frac{2\epsilon\zeta}{\pi r^2 \sigma} \bar{v} .$$

Using some plausible values for the parameters,

$$E \sim \frac{2 \cdot 10^{-11} \cdot 0.1 \cdot 1}{\pi (10^{-4})^2 10^{-4}} \sim 1 \text{ V/m} ,$$

where ζ has been taken as 0.1 V. We found no data on the electrofiltration potentials.

The result might be expected to produce observable effects at the main shock front, at the static water level when the shock reaches that layer or some combination of reflections from the Paleozoics, and at "shock" arrival at the electrodes.

The data obtained by Homuth on Lowball (Appendix F) seem the best to check the concept; those data require more than a dipole source model. A sketch of geologic structure is given in Fig. 7. These data obtained with

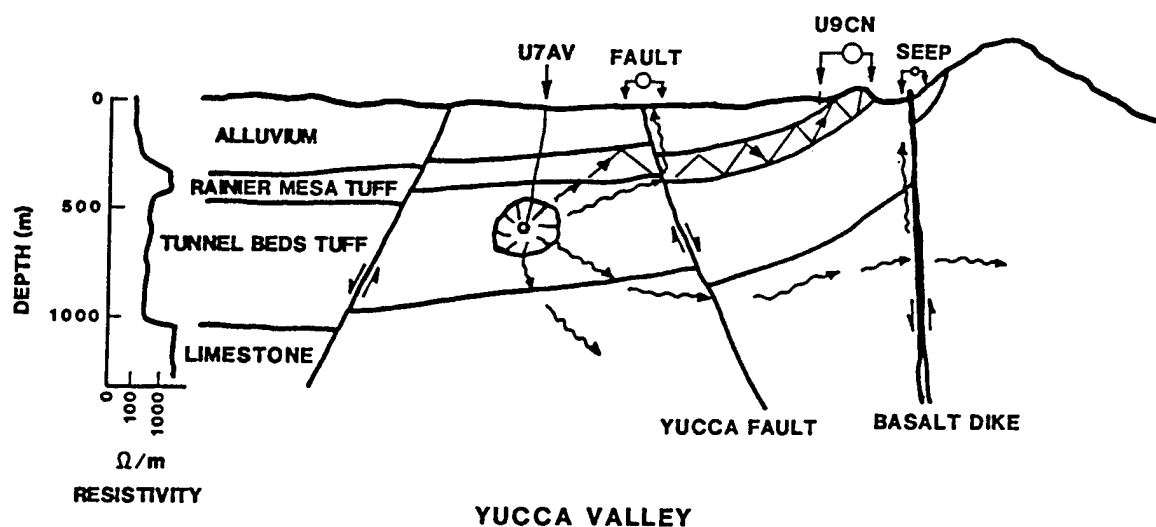


Fig. 7 Geologic influence on EMP signals.

electrodes spanning the Yucca fault at a range of 2.9 km are shown in Figs. 8 and F-1. Average sound velocities in the media are

WP to surface	1.8 km/s
WP region	2.65 km/s
Paleozoic rocks	4.5-6 km/s

The depths of interest are

DOB = 564 m

SWL = 501 m

P_Z = 900 m

Some times of arrival are

WP to SWL	0.024 s
WP to surface	0.31 s
WP to P _Z to SWL	0.28 s
WP to surface to SWL	0.59 s*
WP to P _Z through P _Z to fault	0.77 s*
WP to station	1.60 s
WP to P _Z through P _Z then to SWL	1.19 s*
Slapdown at GZ	1.62 s

Times of appearance of signals from Figs. 8 and F-1 are 0.63, 0.78, 1.0, and 1.1 s. Assuming electrical signals are generated at specific geologic discontinuities and then transmitted as electrical signals to the station, possible regions appear, as noted with asterisks. Better attention to geologic structure and evaluation of shock arrivals would change the values somewhat but there seem to be some correlations.

These and other data are given in the Appendices F and G.

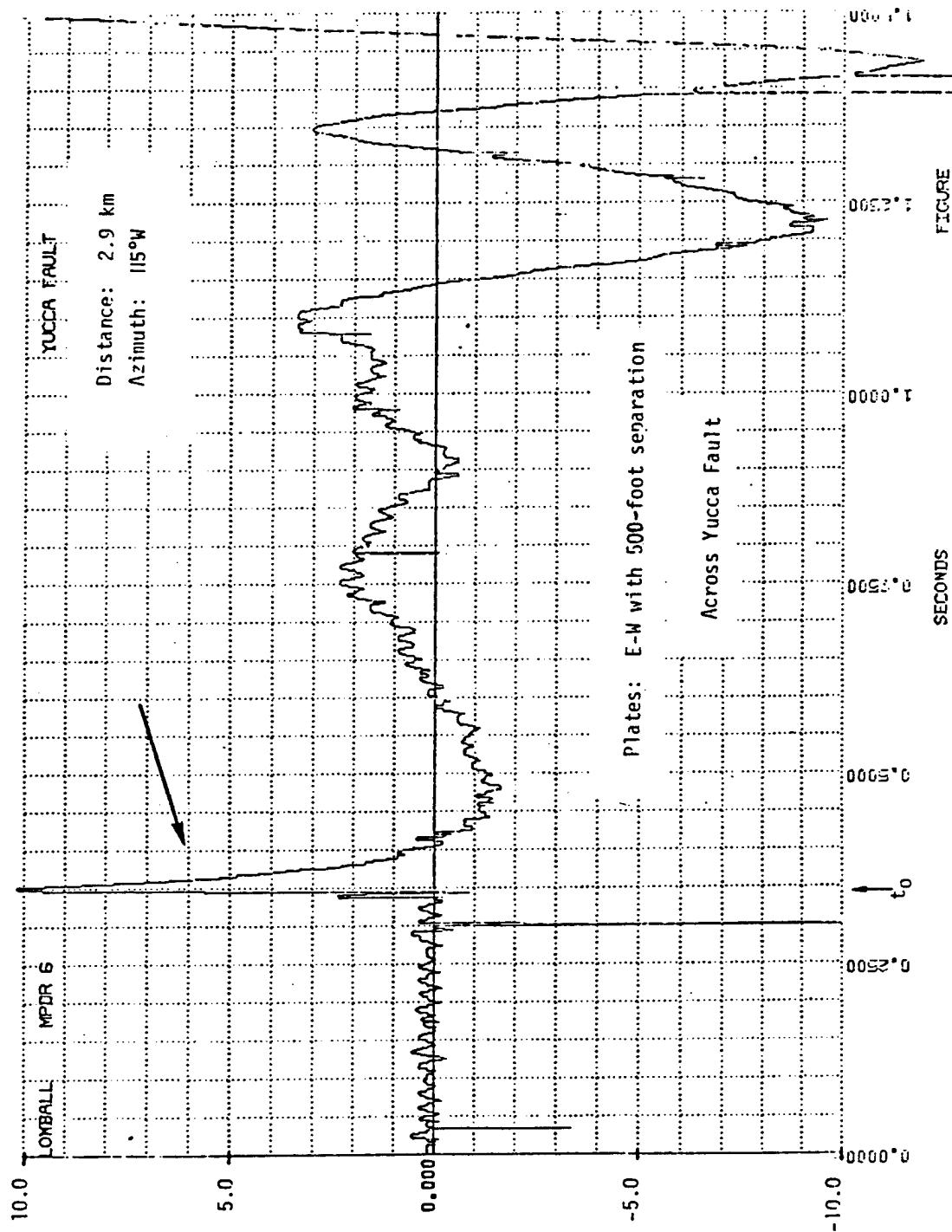


Fig. 8. Yucca fault.

IV. CONCLUSIONS

Considerable data exist for electrical signals emanating from underground nuclear explosions; some, better than others. A definitive explanation of the late-time signals cannot be made at this time. The more probable source of the signals is the seismoelectric effect proposed by Zablocki and Keller.⁹ Data presented here support that explanation, but dipole models cannot be ruled out as contributions. Data from an explosion in a well-characterized medium with measurement of at least radial and azimuthal components of the fields at several azimuths and ranges could probably better delineate the mechanisms. Effort and equipment for such a measurement would be extensive. The signals do not seem useful as a diagnostic tool with present information.

APPENDIX A

EARTH POTENTIAL, MAGNETIC FIELD, AND CABLE CURRENT DATA FROM A LOW-YIELD EVENT (D--) IN ALLUVIUM

Measurements herein were made by R. Fitzhugh. The station locations are shown in Fig. A-1.

Depth of burial	326 m
Diameter of hole	48 in., uncased
Number of cables	~100
Earth conductivity	0.01 to 0.02 S/m

Earth potential plates were of lead, ~2 ft square, and buried to a depth of about 1 m. Typical circuits are given in Fig. A-2. Data are given in Figs. A-3 through A-5.

Magnetic fields were measured with 50-turn coils, 1 m in diameter. Planes of the coils were either vertical or normal to the radius vector to the working point; that is, they measured the vertical and radial magnetic field. These data are given in Figs. A-6 and A-7.

Currents on cables are given in Figs. A-8 and A-9.

The recorder was a multichannel tape deck with ~40-kHz bandwidth. Polarities may be uncertain in some cases.

A summary of these data is given in Table A-I.

TABLE A-I
SUMMARY OF DATA FROM THE LOW-YIELD EVENT D--

<u>Fitzhugh's Data</u>						
<u>Orientation</u>	<u>Location</u>	<u>Fig. No.</u>	<u>R(m)</u>	<u>Field</u>	<u>Conversion</u>	<u>Peak</u>
D--:						
NS	W	A-3	480	$-E_{\phi}$	-0.0164	+0.44
EW	W	A-3	480	$+E_R$	+0.0164	-0.50
NS	E	A-4	415	$-E_{\phi}$	-0.0164	+0.04
EW	E	A-4	415	$-E_R$	-0.0164	+0.44
NS	S	A-5	225	$-E_R$	-0.0164	+0.44
EW	S	A-5	225	$-E_{\phi}$	-0.0082	+0.25
Normal	S	A-6	225	$\begin{vmatrix} \dot{B}_R \\ \dot{B}_{\phi} \end{vmatrix}$	255	11 g/s
Vertical	S	A-7	225	$\begin{vmatrix} \dot{B}_R \\ \dot{B}_{\phi} \end{vmatrix}$	255	8 g/s

Inlet:

EW	N	6	1054	$-E_{\phi}$	-0.0164	+0.024
NS	N	3	1054	$-E_R$	-0.0164	+0.032

Diffusion Times: ($\sigma = 0.01$ S/m)

<u>Station</u>	<u>Distance (m)</u>	<u>$\tau = \mu\sigma r^2/4$ (ms)</u>
D--:		
GZ	326	0.334
West	580	1.06
East	516	0.84
South	375	0.44

Inlet:

GZ	818	2.1
North	1334	5.6

D--: The E_{ϕ} at the W and E locations ought to be zero, as should the E_R at the S location if MD.

Inlet: E_R ought to be zero at the N location.

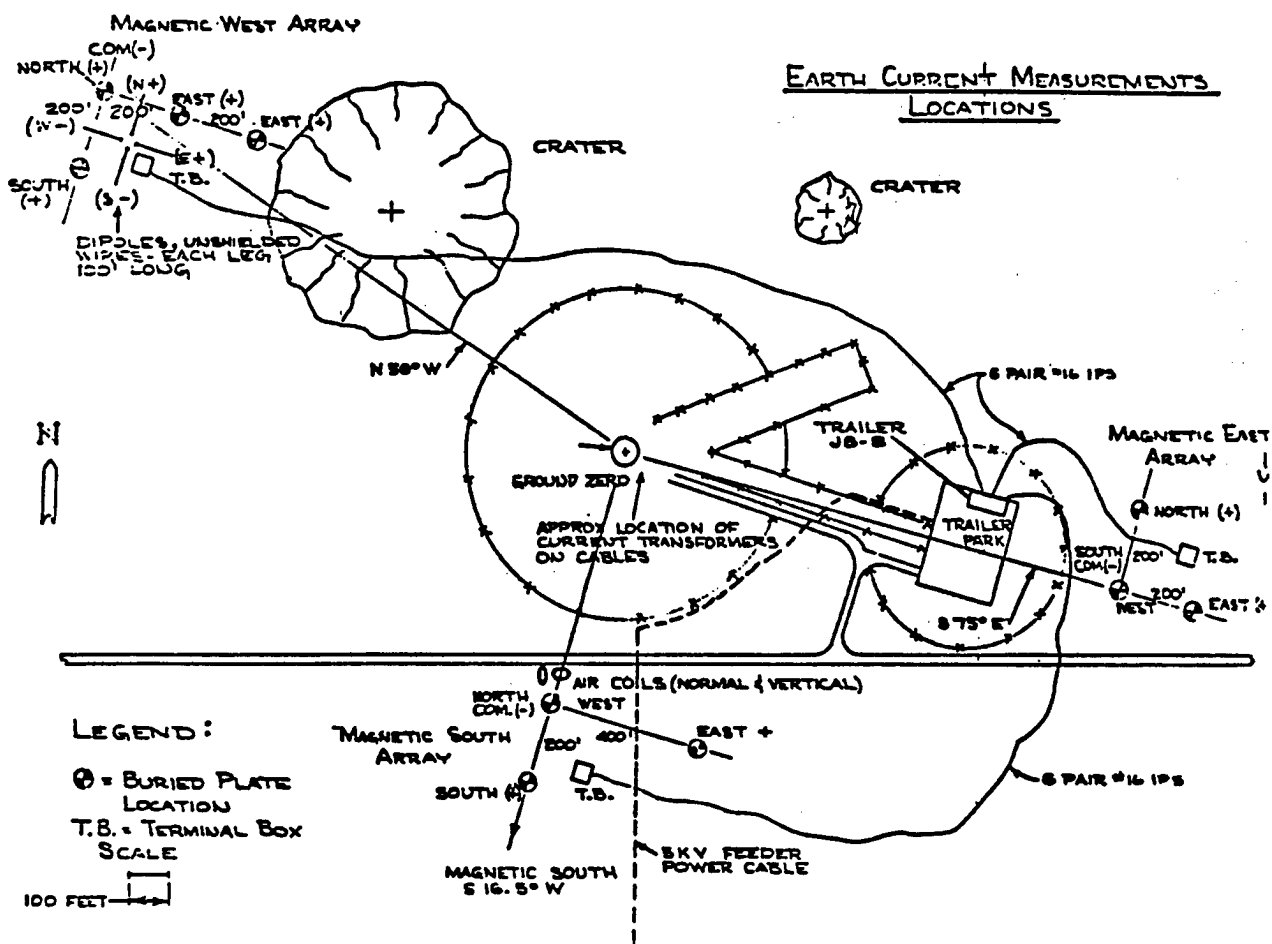


Fig. A-1. Station layout for the low-yield event D--.

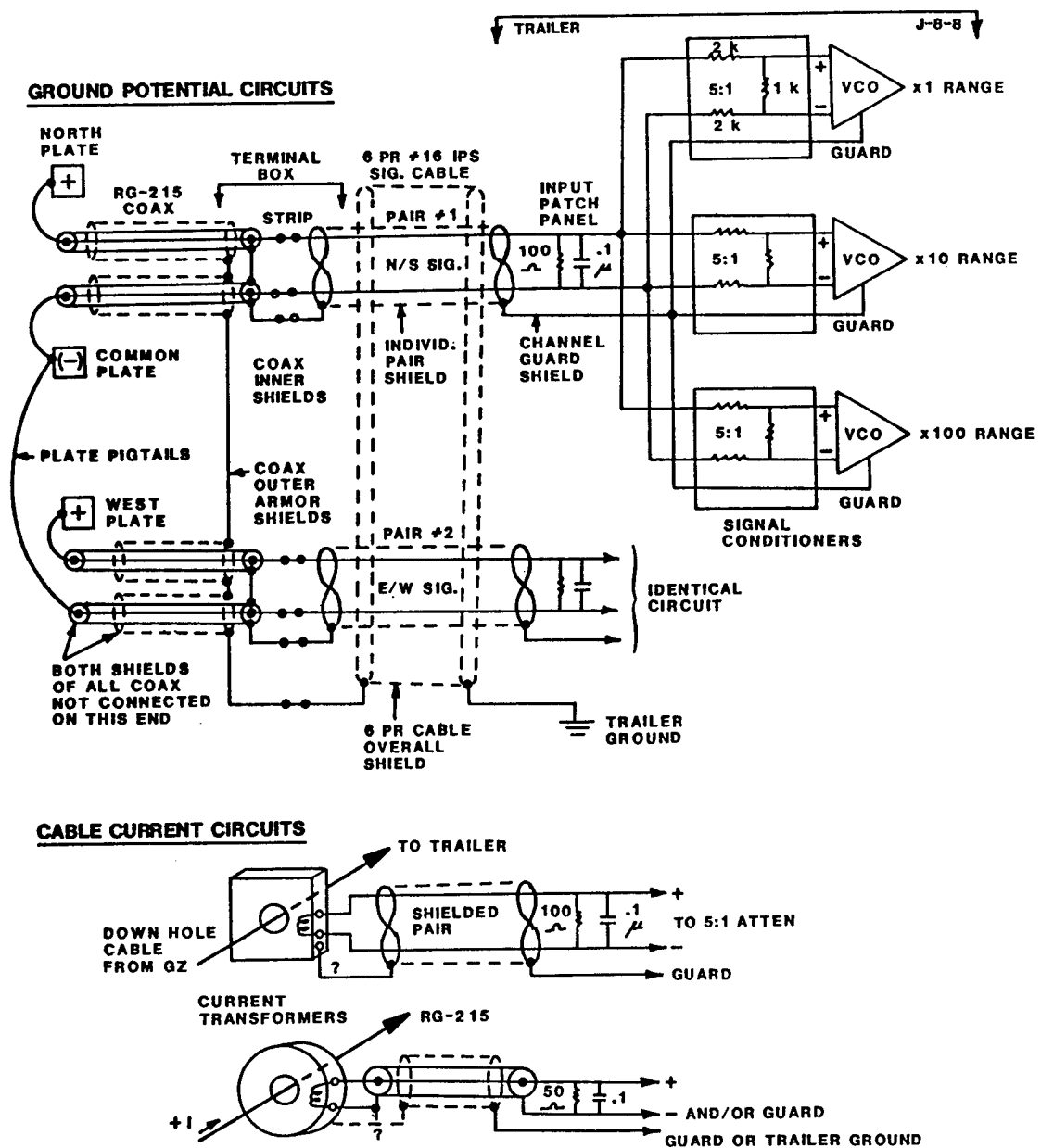


Fig. A-2. Typical differential circuits for earth-current measurements.

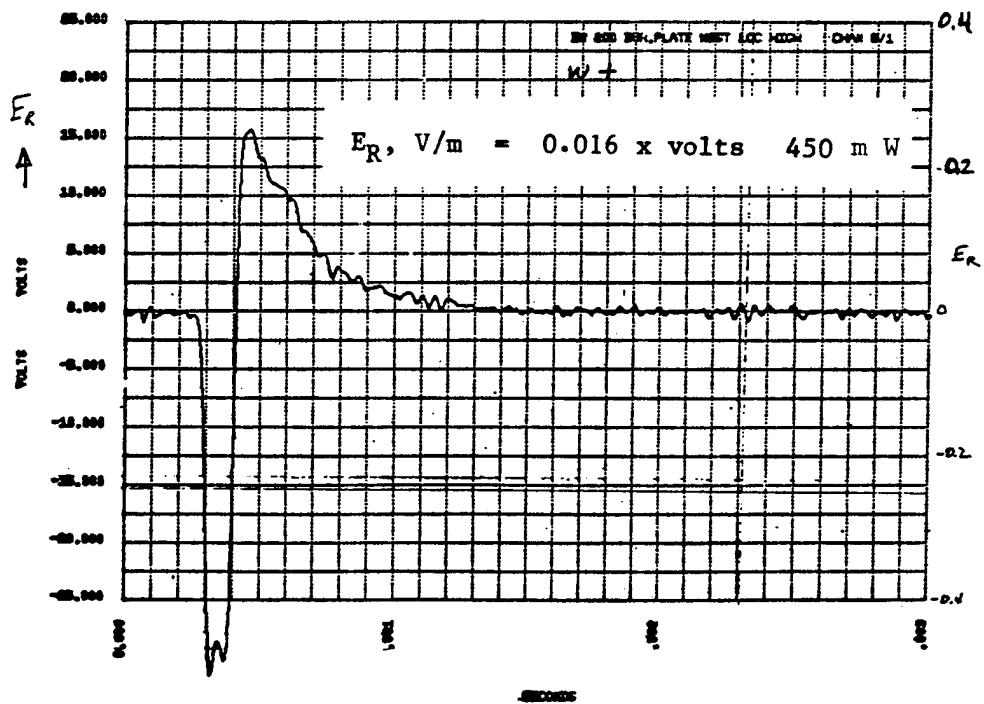
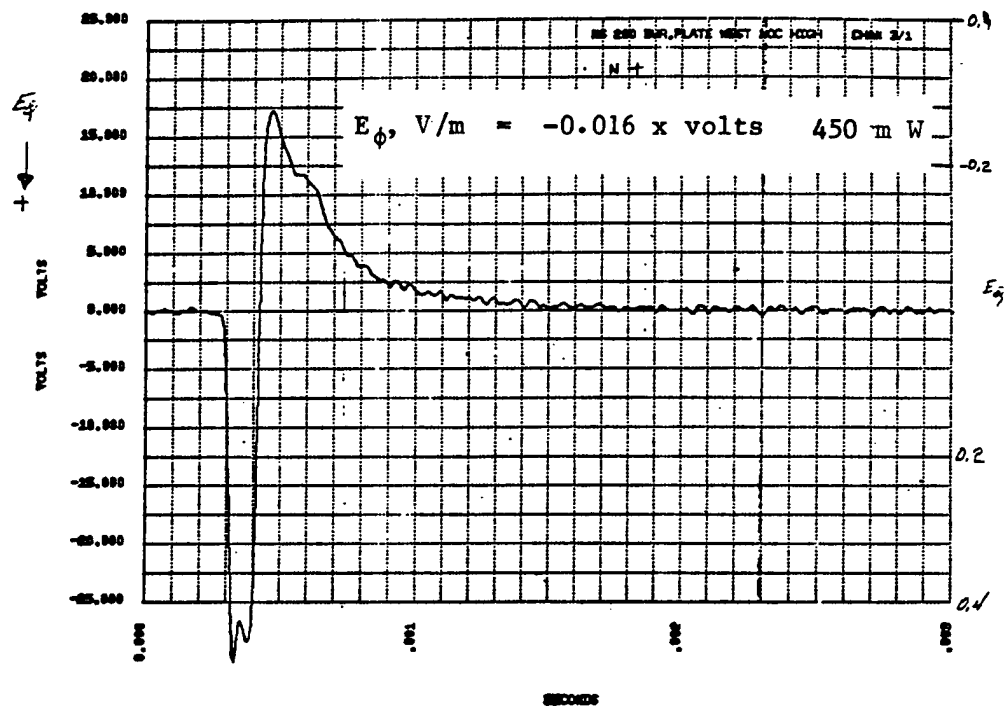


Fig. A-3. Data from west location: upper, N-S plates; lower, E-W plates.

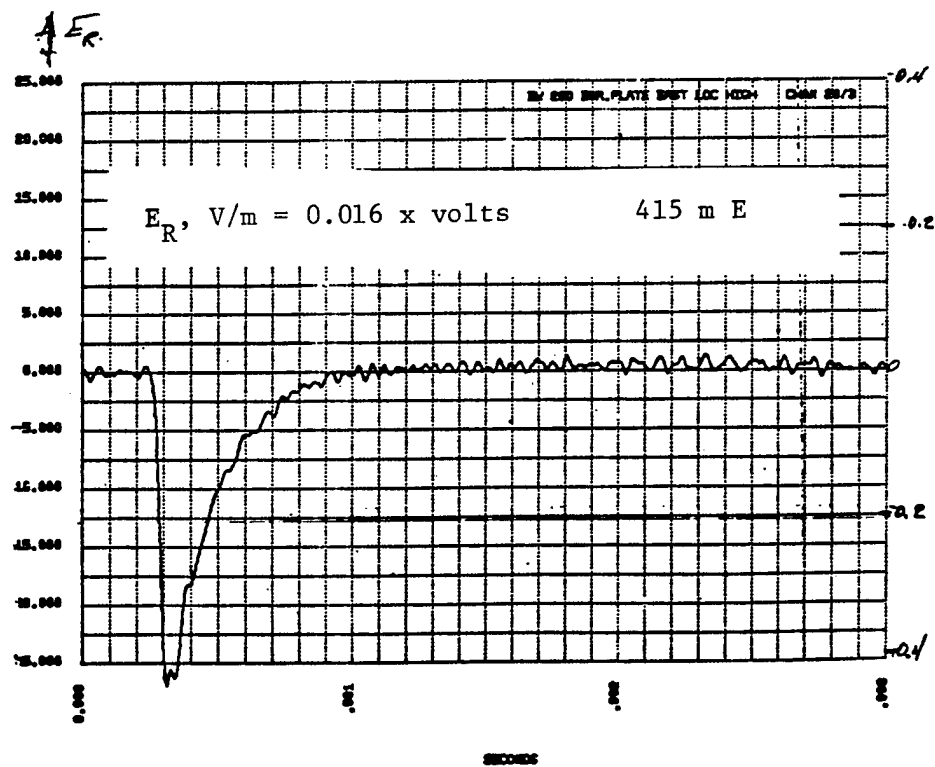
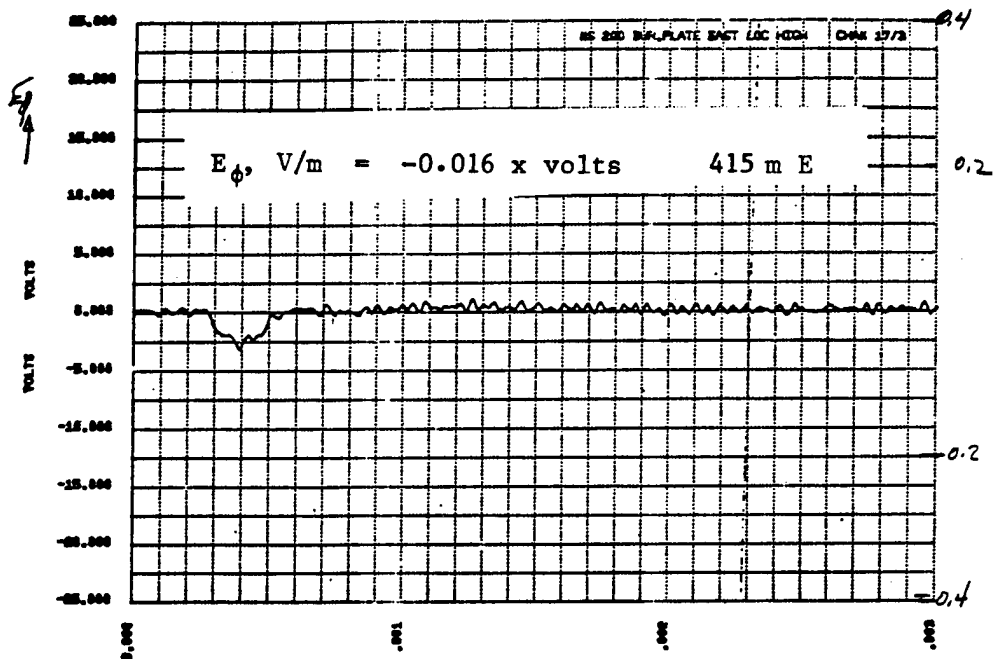


Fig. A-4. Data from east location: upper, N-S plates; lower, E-W plates.

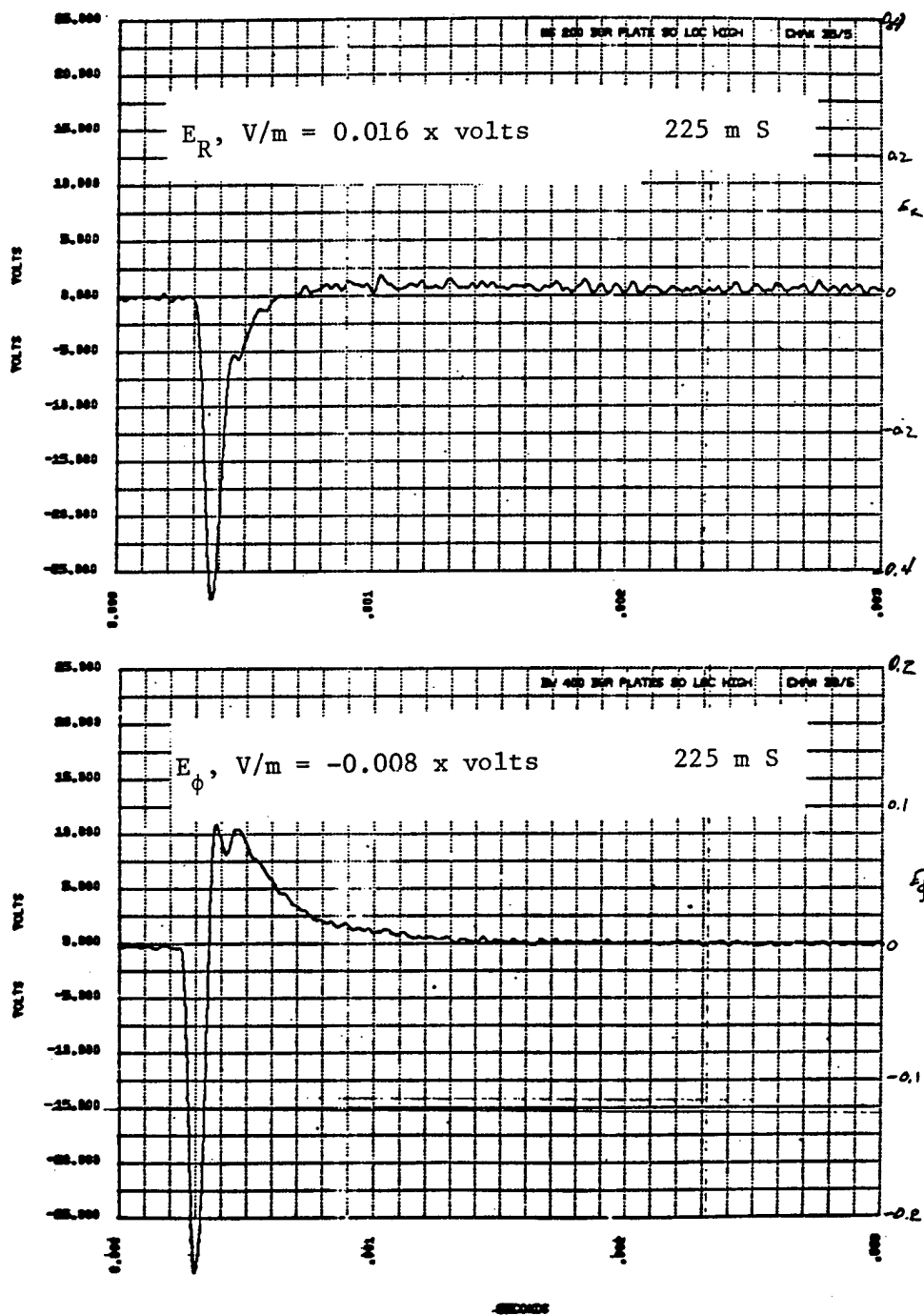


Fig. A-5. Potential data from south location: upper, N-S plates; lower, E-W plates.

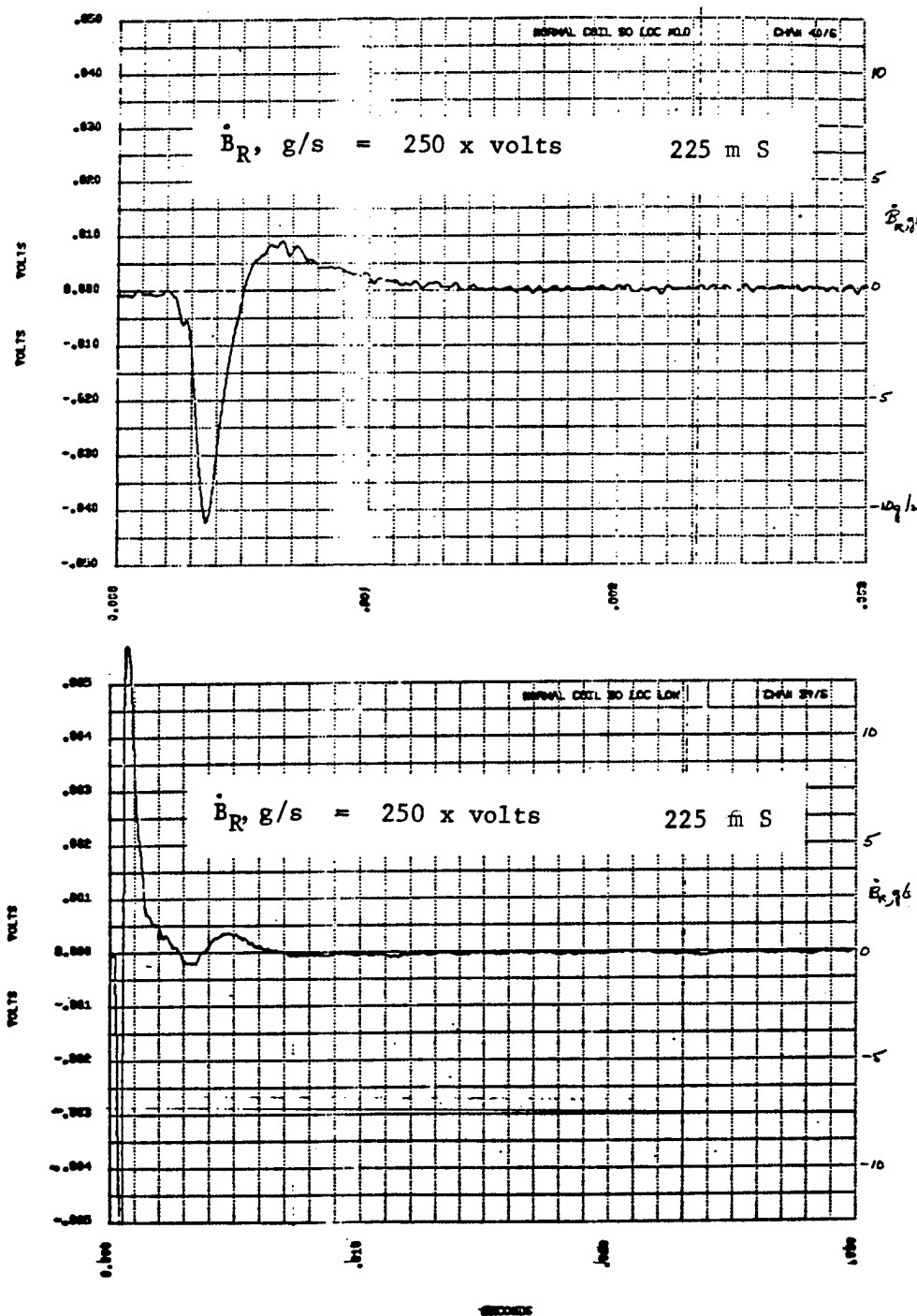


Fig. A-6. Radial magnetic field from south location.

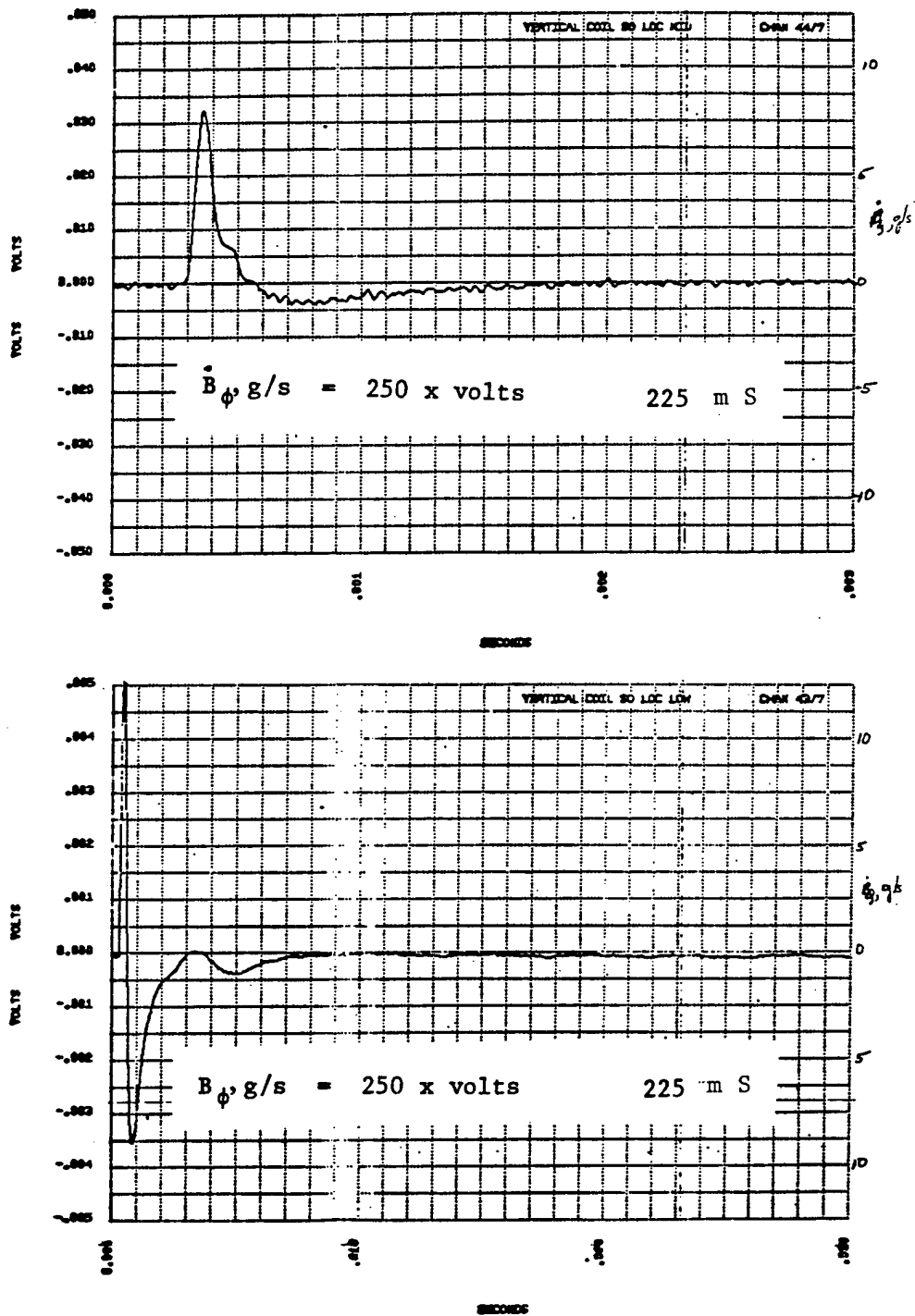


Fig. A-7. Azimuthal magnetic field from south location.

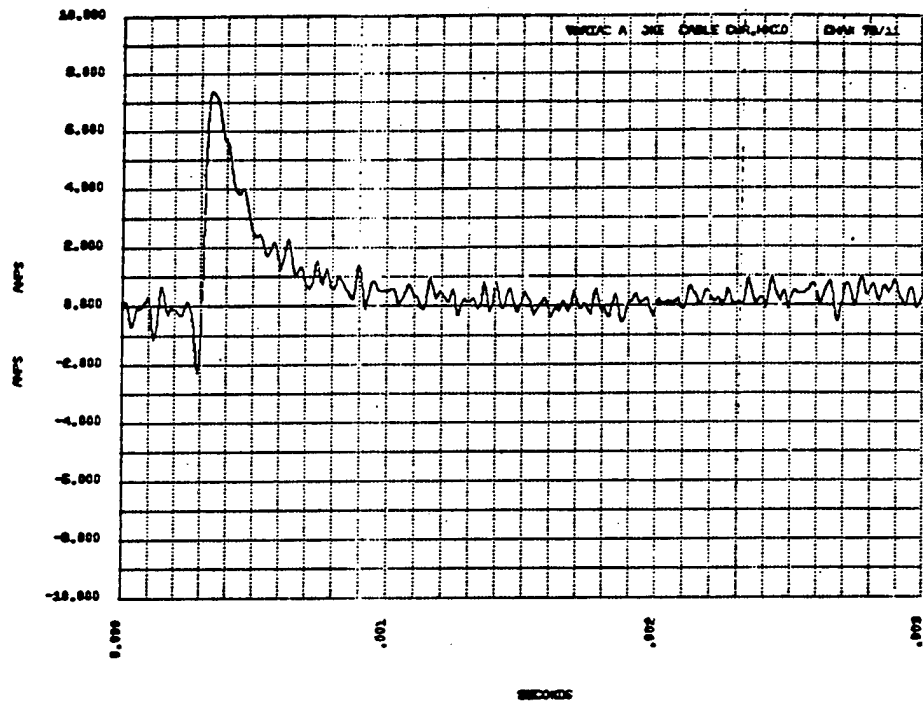


Fig. A-8. Current on single signal cable.

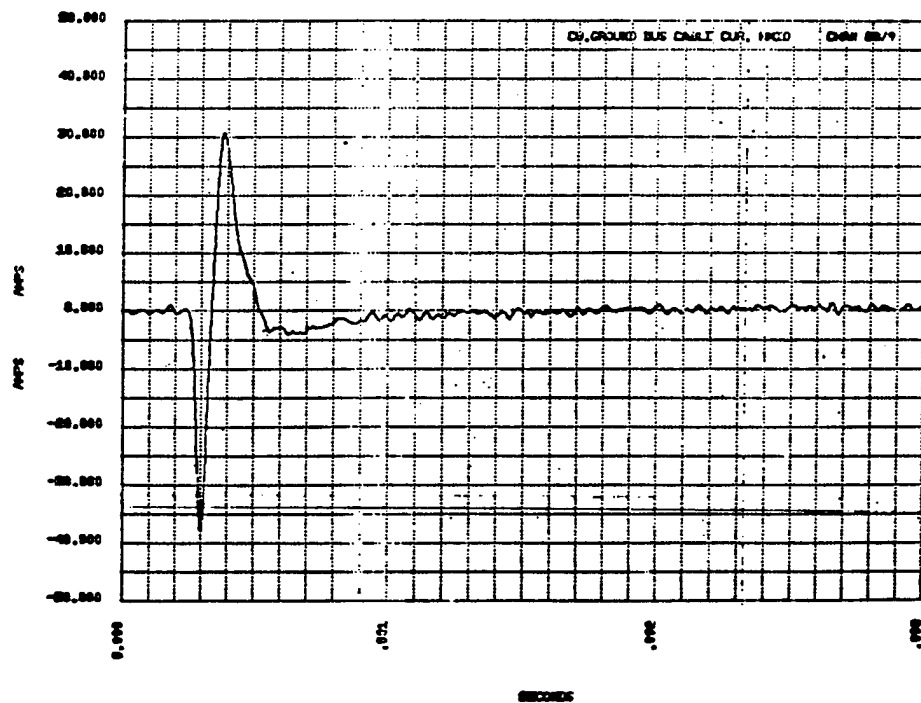


Fig. A-9. Current on ground bus.

APPENDIX B

USEFUL LAPLACE TRANSFORMS AND MODIFIED BESSEL FUNCTION RELATIONS

I. LAPLACE TRANSFORMS

<u>f(s)</u>	<u>F(t)</u>	<u>Ref. No.*</u>
$e^{-k\sqrt{s}}$	$\frac{k}{2\sqrt{\pi t^3}} \exp\left(-\frac{k^2}{4t}\right)$	#82
$\sqrt{s} e^{-k\sqrt{s}}$	$\frac{1}{2\sqrt{\pi t^3}} \left(\frac{k^2}{2t} - 1\right) e^{-k^2/4t}$	--
$\frac{1}{s} e^{-k\sqrt{s}}$	$\operatorname{erfc}\left(\frac{k}{2\sqrt{t}}\right)$	#83
$\frac{1}{\sqrt{s}} e^{-k\sqrt{s}}$	$\frac{1}{\sqrt{\pi t}} e^{-k^2/4t}$	#84
$s^{-3/2} e^{-k\sqrt{s}}$	$2\sqrt{\frac{t}{\pi}} e^{-k^2/4t} - k \operatorname{erfc}\left(\frac{k}{2\sqrt{t}}\right)$	#85

*Transform number from Standard Mathematical Tables, 12th Ed. (Chemical Rubber Publishing Company, Cleveland, Ohio, 1956).

II. ASYMPTOTIC EXPANSIONS OF MODIFIED BESSEL FUNCTION RELATIONS FOR LARGE X

$$I_0(x) \approx \frac{e^x}{\sqrt{2\pi x}} \left(1 + \frac{1}{8x} + \frac{9}{2!(8x)^2} + \dots \right)$$

$$I_1(x) \approx \frac{e^x}{\sqrt{2\pi x}} \left(1 - \frac{3}{8x} - \frac{15}{2!(8x)^2} - \dots \right)$$

$$K_0(x) \approx \sqrt{\frac{\pi}{2x}} e^{-x} \left(1 - \frac{1}{8x} + \frac{9}{2!(8x)^2} + \dots \right)$$

$$K_1(x) \approx \sqrt{\frac{\pi}{2x}} e^{-x} \left(1 + \frac{3}{8x} - \frac{15}{2!(8x)^2} + \dots \right) .$$

Relations for derivatives of modified Bessel functions:

$$I_0'(x) = I_1(x)$$

$$K_0'(x) = -K_1(x) .$$

APPENDIX C
SCALING RELATIONS FOR UNDERGROUND NUCLEAR EXPLOSIONS

Cavity Radii

Dry alluvium	$17 W^{1/3} \text{ m}$
Dry tuff	$15 W^{1/3} \text{ m}$
Saturated tuff	$(13 \text{ to } 15) W^{1/3} \text{ m}$
Rhyolite	$(9 \text{ to } 11) W^{1/3} \text{ m}$

Melt Radius

$$4 W^{1/3} \text{ m}$$

Vaporization Radius

$$2 W^{1/3} \text{ m}$$

CEP Formula for Cavity Radius

$$R_c = \frac{70.2 W^{1/3}}{(\rho h)^{1/4}} \text{ m}$$

(h in meters, ρ in Mg/m^3)

Early Cavity Radius Growth

$$R_c = 7 W^{0.2} t^{0.5} \text{ m}$$

(t in ms)

Note: In all the above formulae, W is in kilotons.

See Fig. C-1 for plots of radius vs time for a 1-kt explosion at 675 m in alluvium.

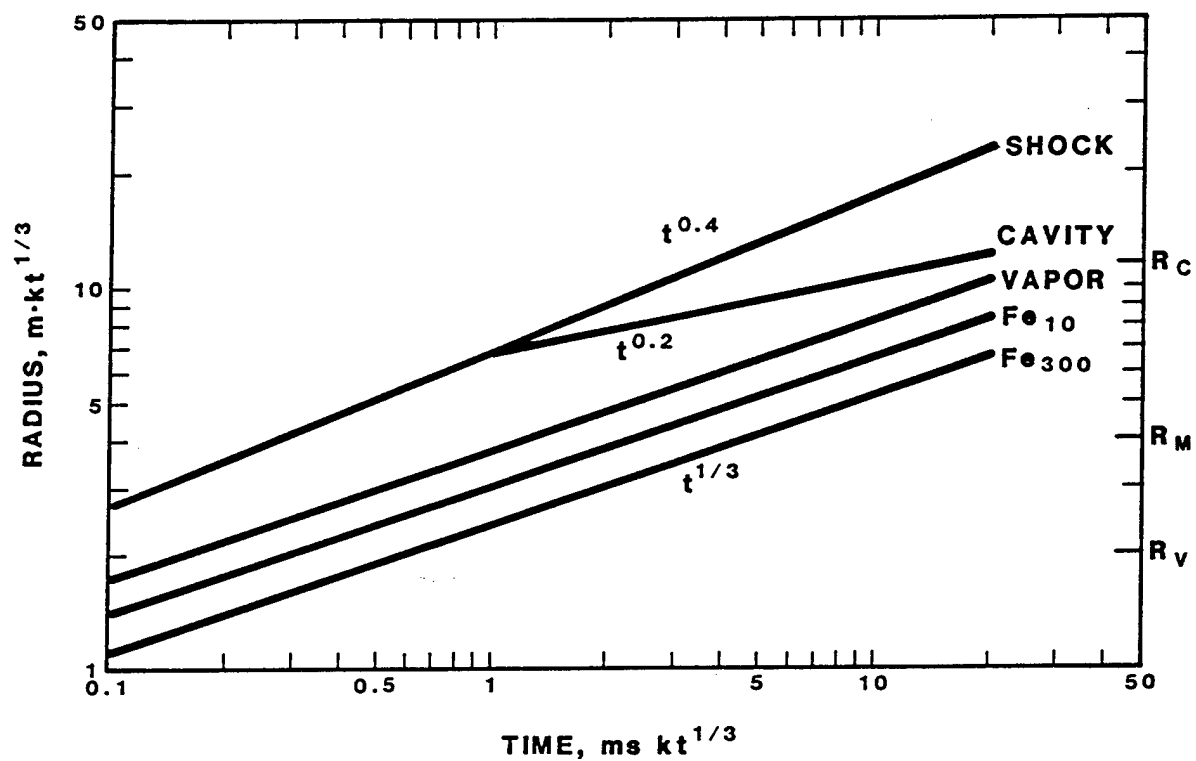


Fig. C-1. Radii vs time for a 1-kt explosion at 675 m in alluvium. Scaled from 10- and 300-kt calculations by T. Cook of Los Alamos. Initial conditions: energy in 1-m-radius iron gas sphere of mass 6 Mg.

$$t = t_1 W^{1/3}$$

$$r = r_1 W^{1/3}$$

APPENDIX D

GEOLOGIC SETTING FOR EVENT LOWBALL

TABLE D-I

PHYSICAL PROPERTY SUMMARY

Hole: U7av

Event: LOWBALL

<u>Physical Property</u>	<u>Depth (m)</u>	<u>Data Averages</u>
1. Average Overburden Density	WP to surface	1.88 Mg/m ³
2. Average Density*	WP +21.3,-61.0	1.91 Mg/m ³
3. Grain Density	WP + 21.3,-61.0	2.47 Mg/m ³
4. Average Seismic Velocity	WP to surface	1807 m/s
5. Average Seismic Velocity	WP +0,-61.0	2649 m/s
6. Average Water Content	WP +21.3,-61.0	21.4/22.7%**
7. Porosity	WP +21.3,-61.0	39/40%**
8. Saturation	WP +21.3,-61.0	104/108%**
9. Gas-Filled Porosity	WP +21.3,-61.0	-1/-3%**
10. Average CO ₂ Content ²	WP +21.3,-61.0	<0.5%
11. Depths and Per Cent of Swelling Clay: <10% montmorillonite		

*H₂O corrected.

**Water bias removed/raw data.

†Propagated error.

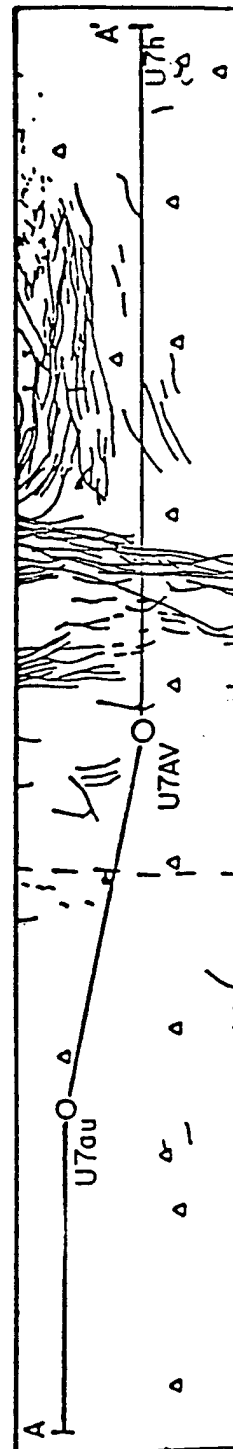
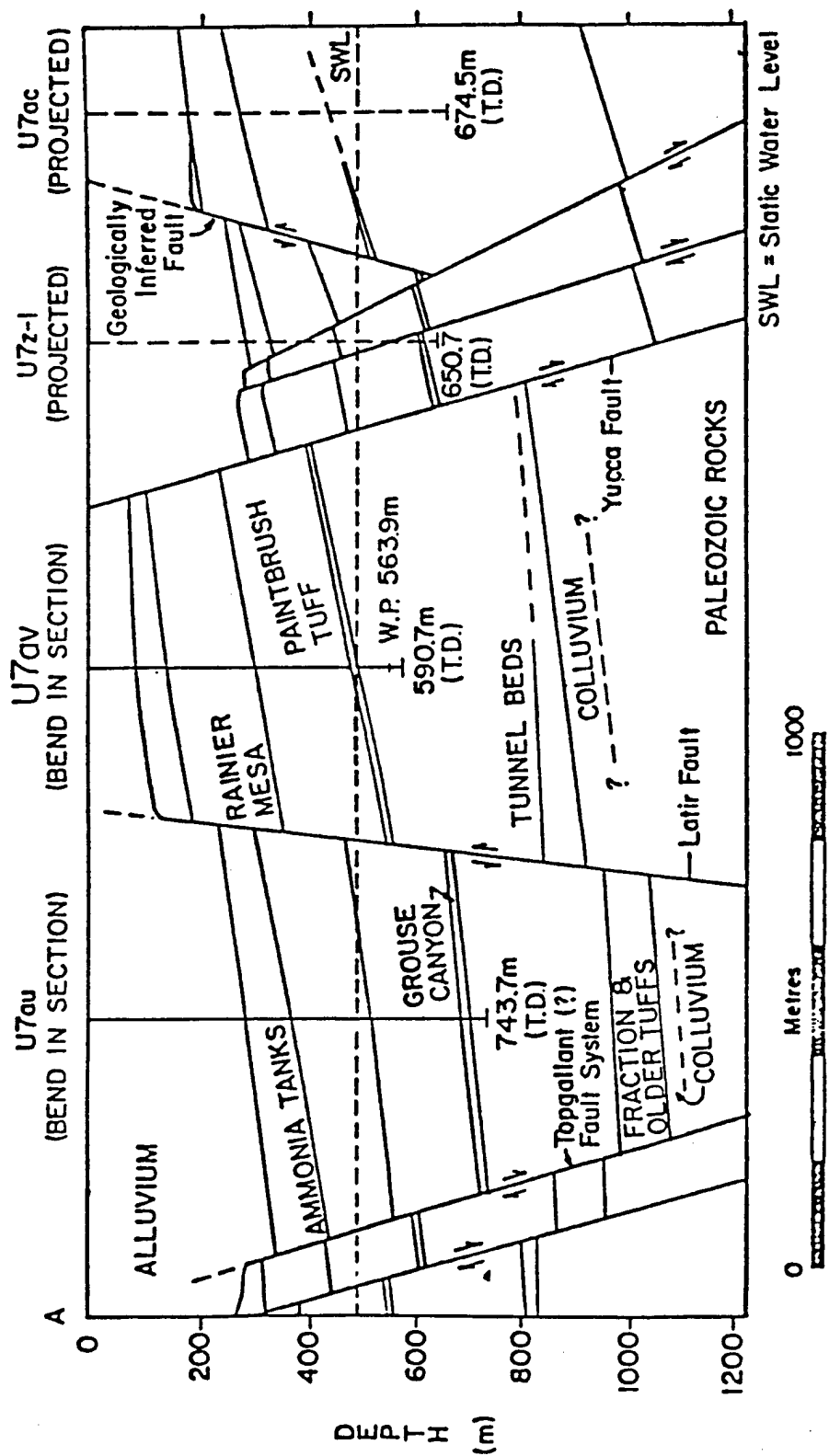


Fig. D-1. E-W geologic cross section through U7av.

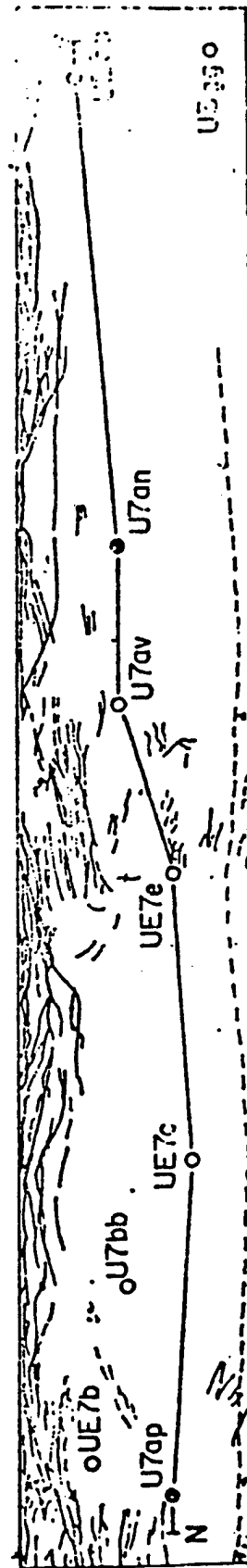
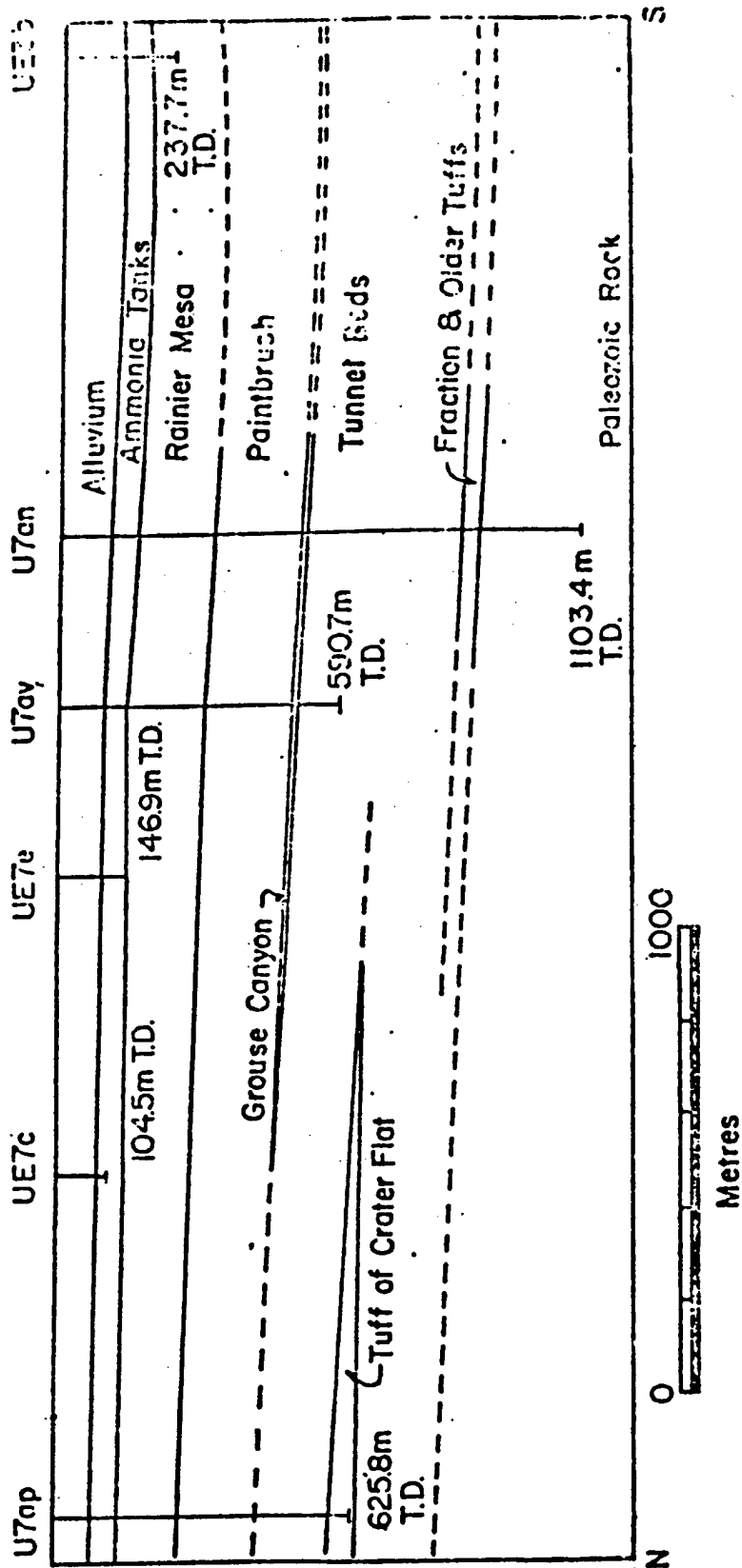


Fig. D-2. N-S geologic cross section through U7av.

APPENDIX E

EARTH MOTION DATA OBTAINED BY R. FITZHUGH FROM EVENT LOWBALL

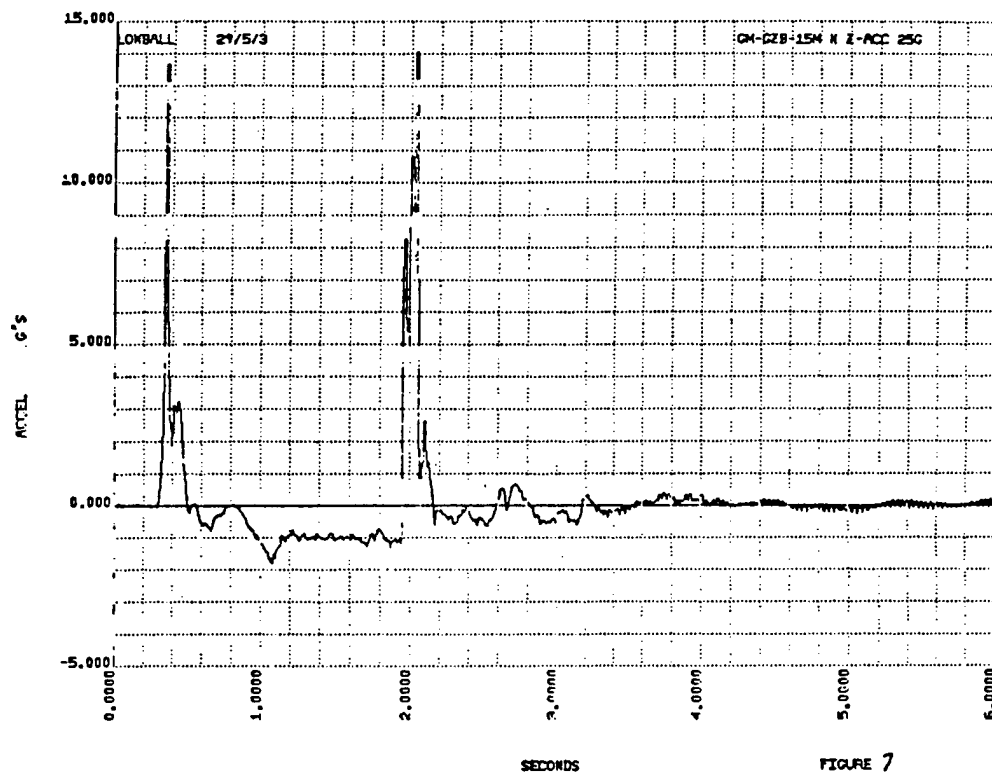


FIGURE 7

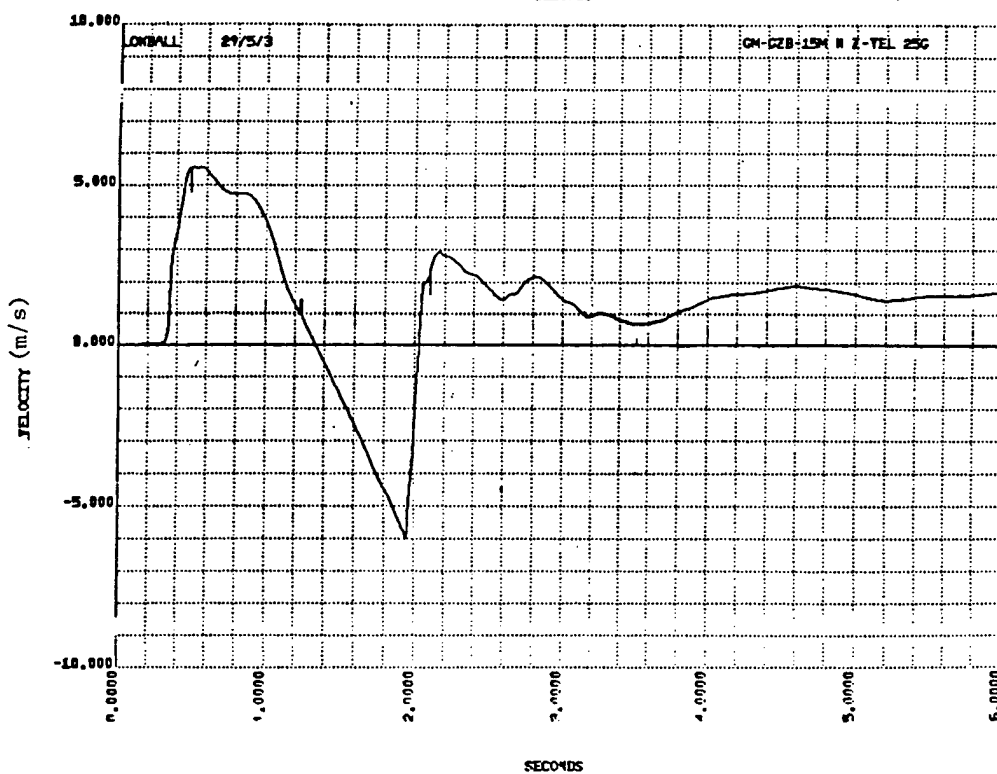


Fig. E-1. Earth motion data. Acceleration in g's vs t and velocity in m/s vs t at 15 m from ground zero.

APPENDIX F

DATA OBTAINED BY F. HOMUTH ON UNDERGROUND EVENTS

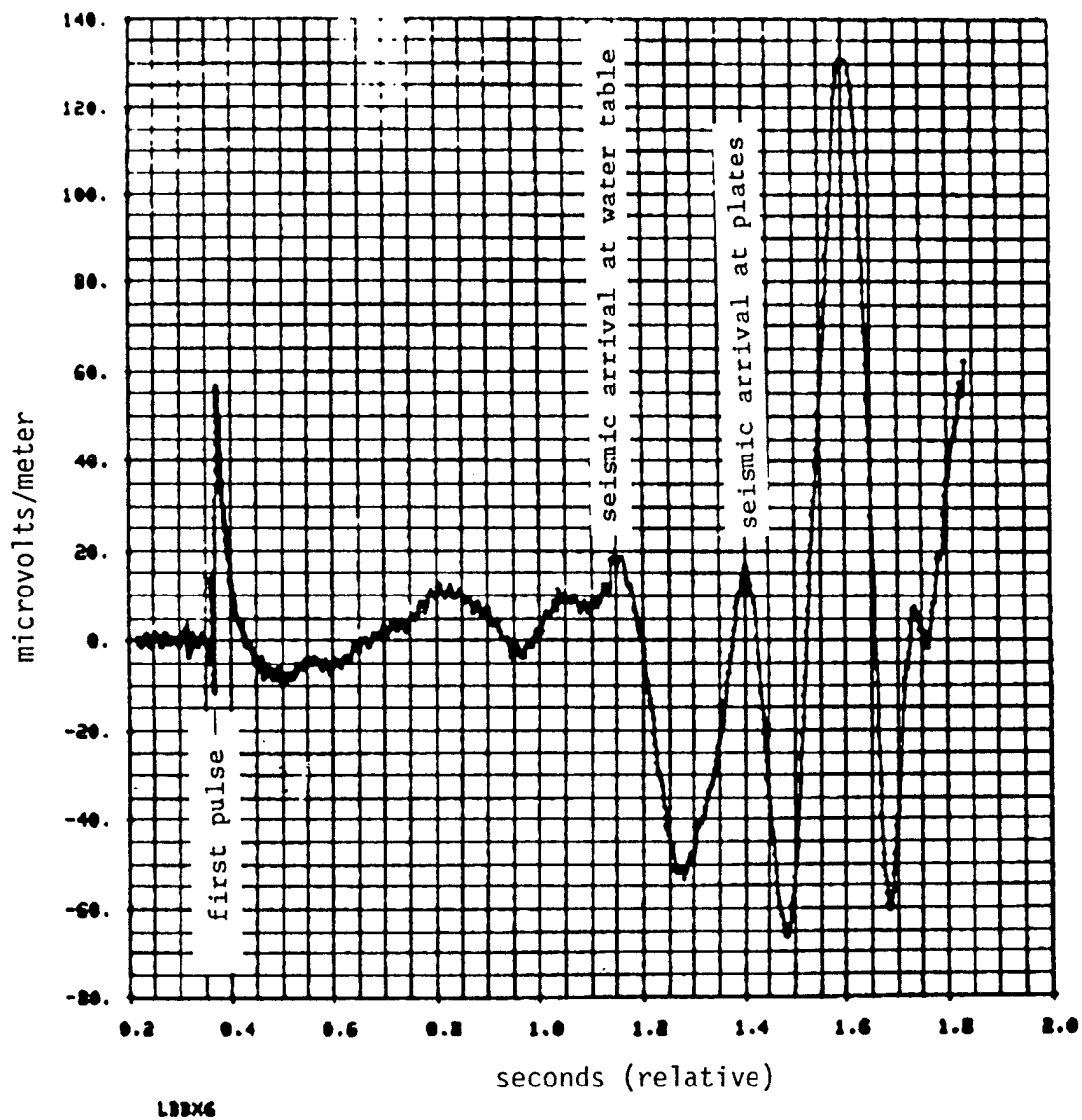


Fig. F-1. Lowball Event EMP--Buried plates across Yucca fault.

Distance: 2.9 km

Azimuth from GZ: N5°W

Plate Separation: 150 m

Plate Orientation: E-W

(Tangential)

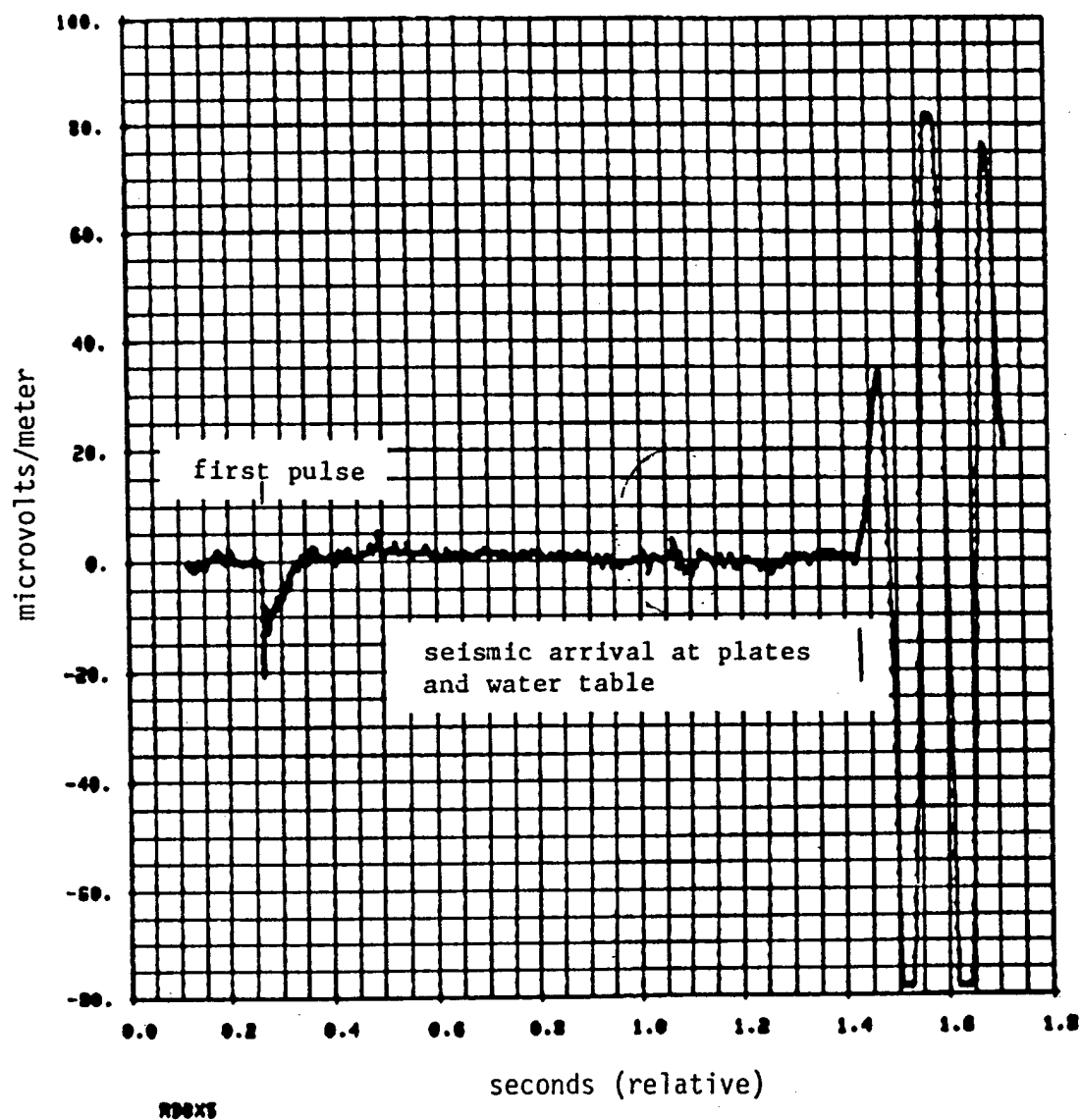
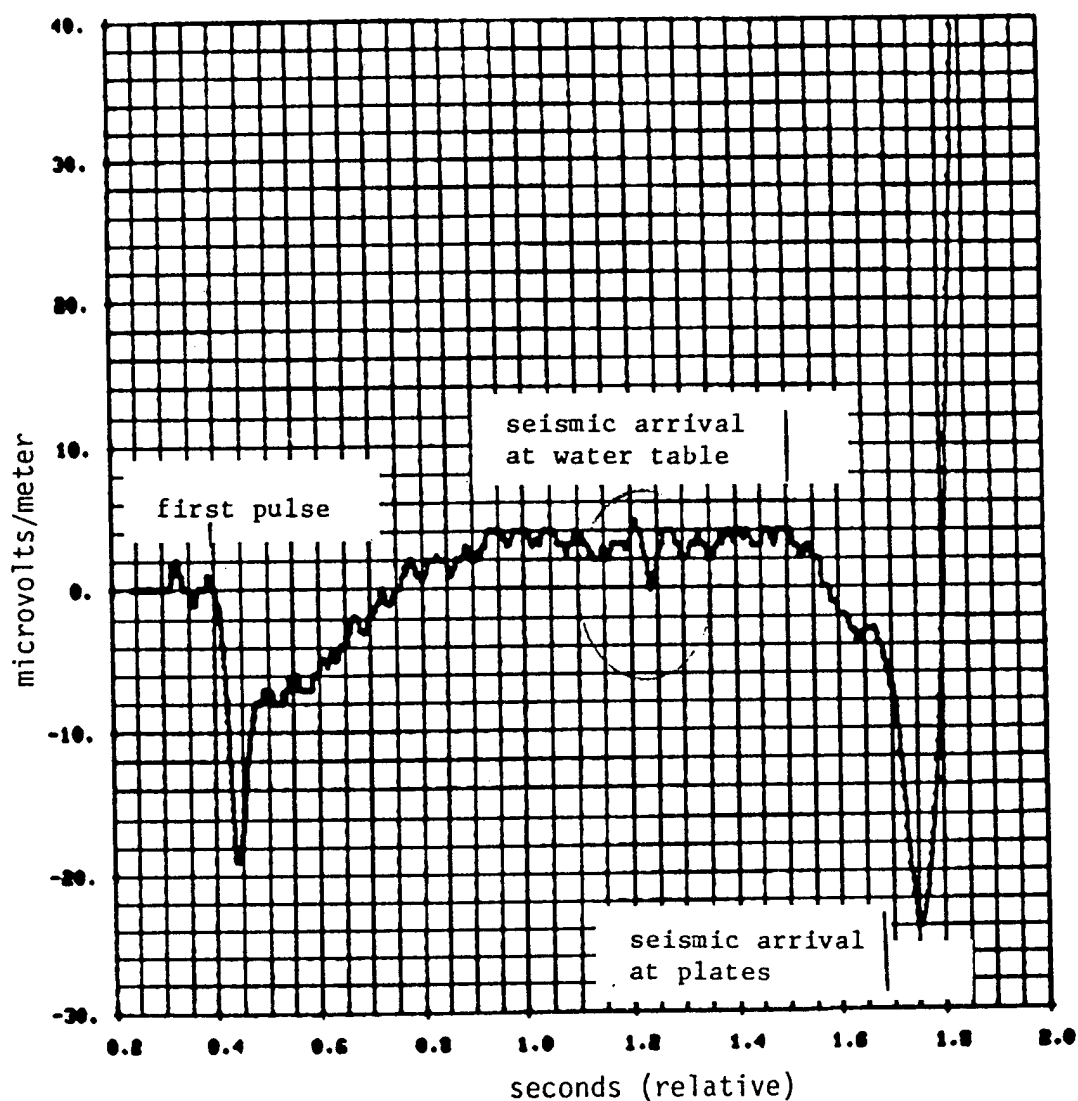


Fig. F-2. Draughts Event EMP--Buried plates near seep.

Distance: 4.7 km
 Azimuth from GZ: N64°E
 Plate Separation: 30 m
 Plate Orientation: N35W



R06X8

Fig. F-3. Rummy Event EMP--Plates in drill hole UelK.

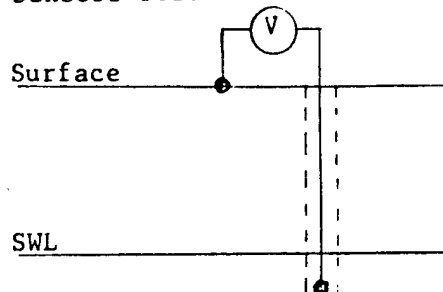
Distance: 4.7 km

Azimuth from GZ: S7°W

Place Separation: 494 m

Plate Orientation: Vertical

Sensors below water table



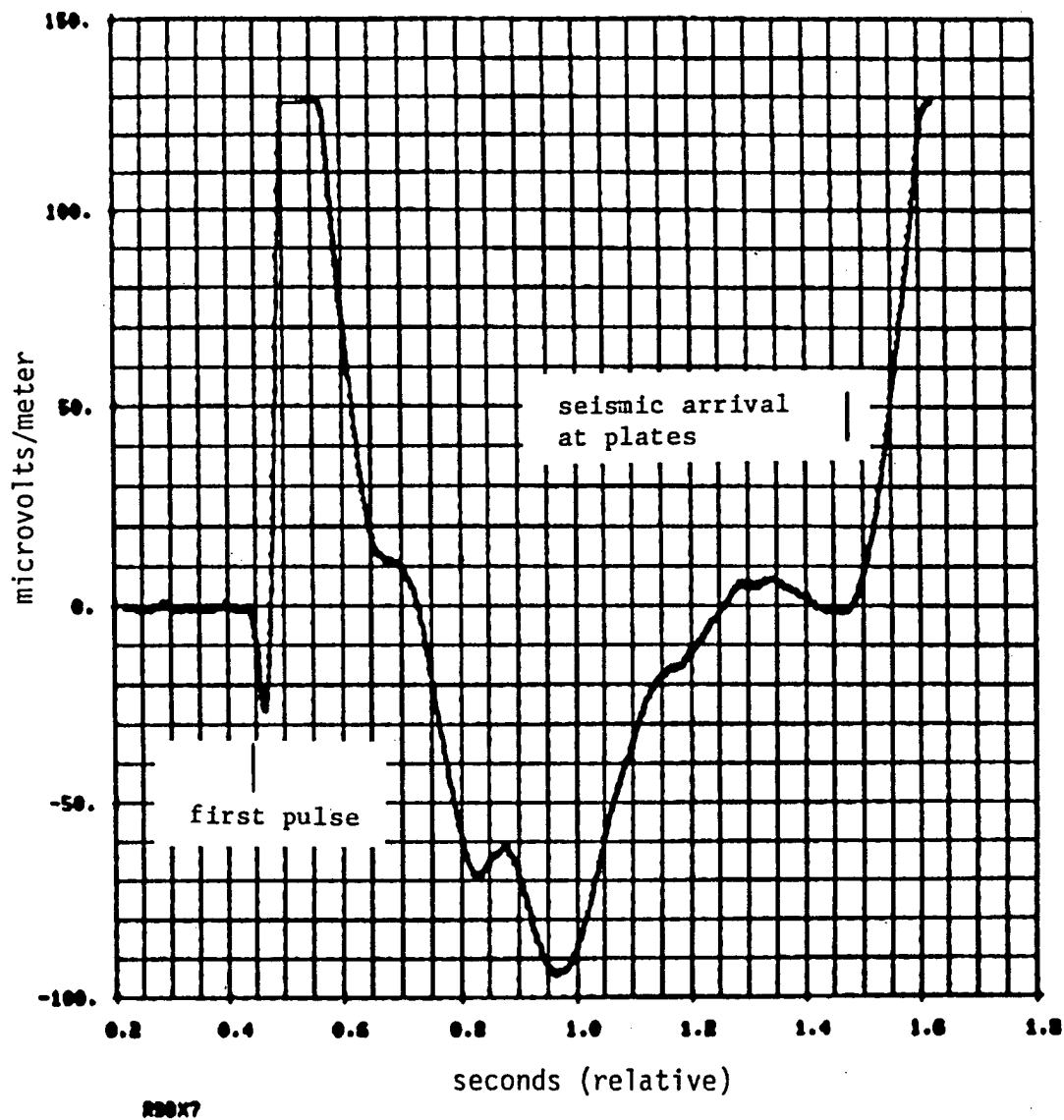


Fig. F-4. Draughts Event EMP--Plates in drill hole UelK.

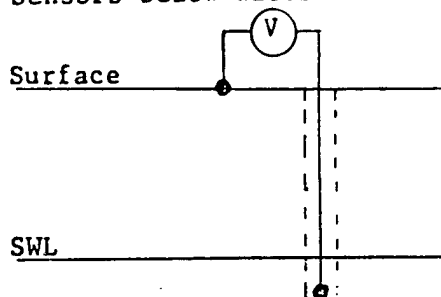
Distance: 5.2 km

Azimuth from GZ: S39°W

Plate Separation: 555 m

Plate Orientation: Vertical

Sensors below water table



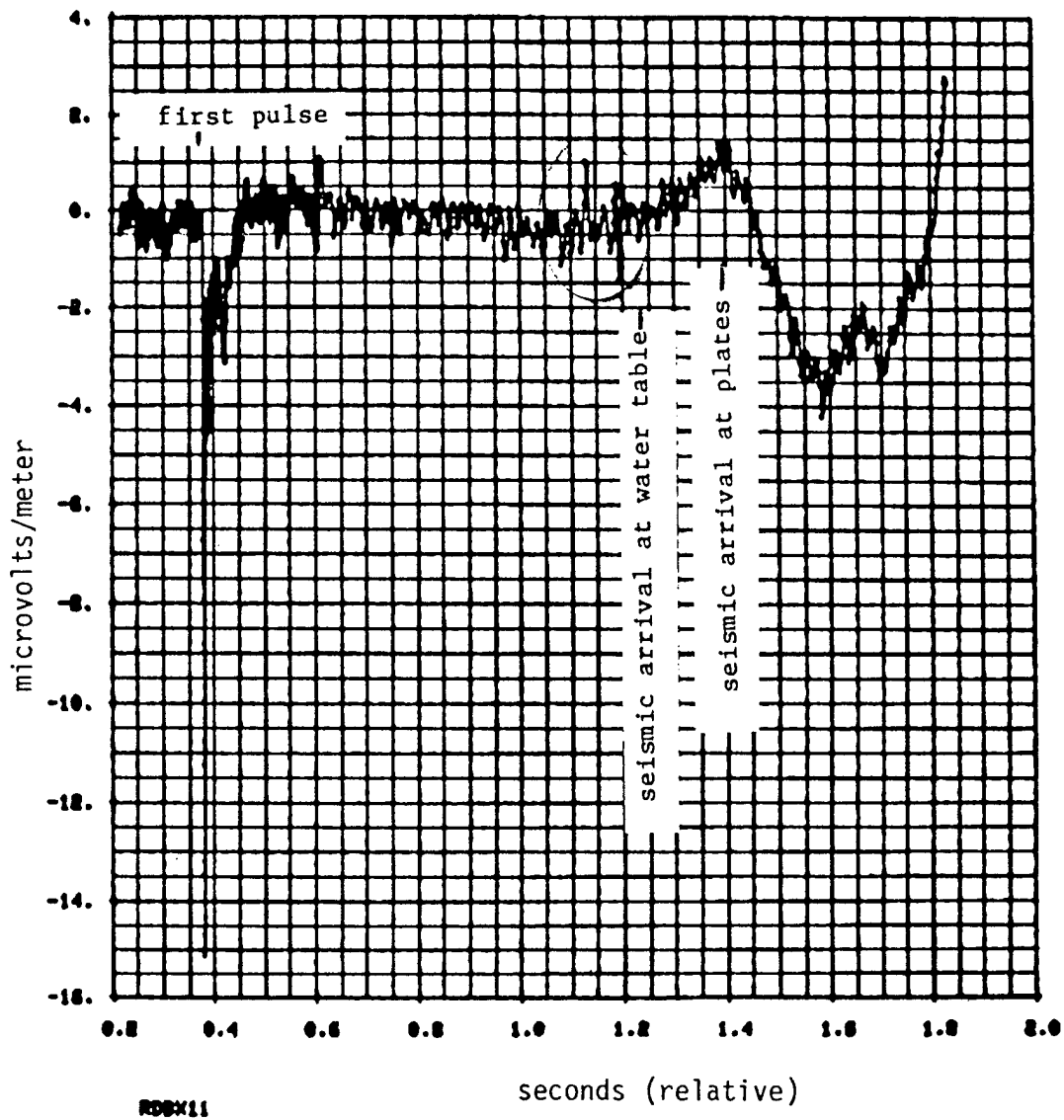


Fig. F-5. Draughts Event EMP--Buried plates across Yucca fault.
 Distance: 4.1 km
 Azimuth from GZ: N33°W
 Plate Separation: 150 m
 Plate Orientation: E-W

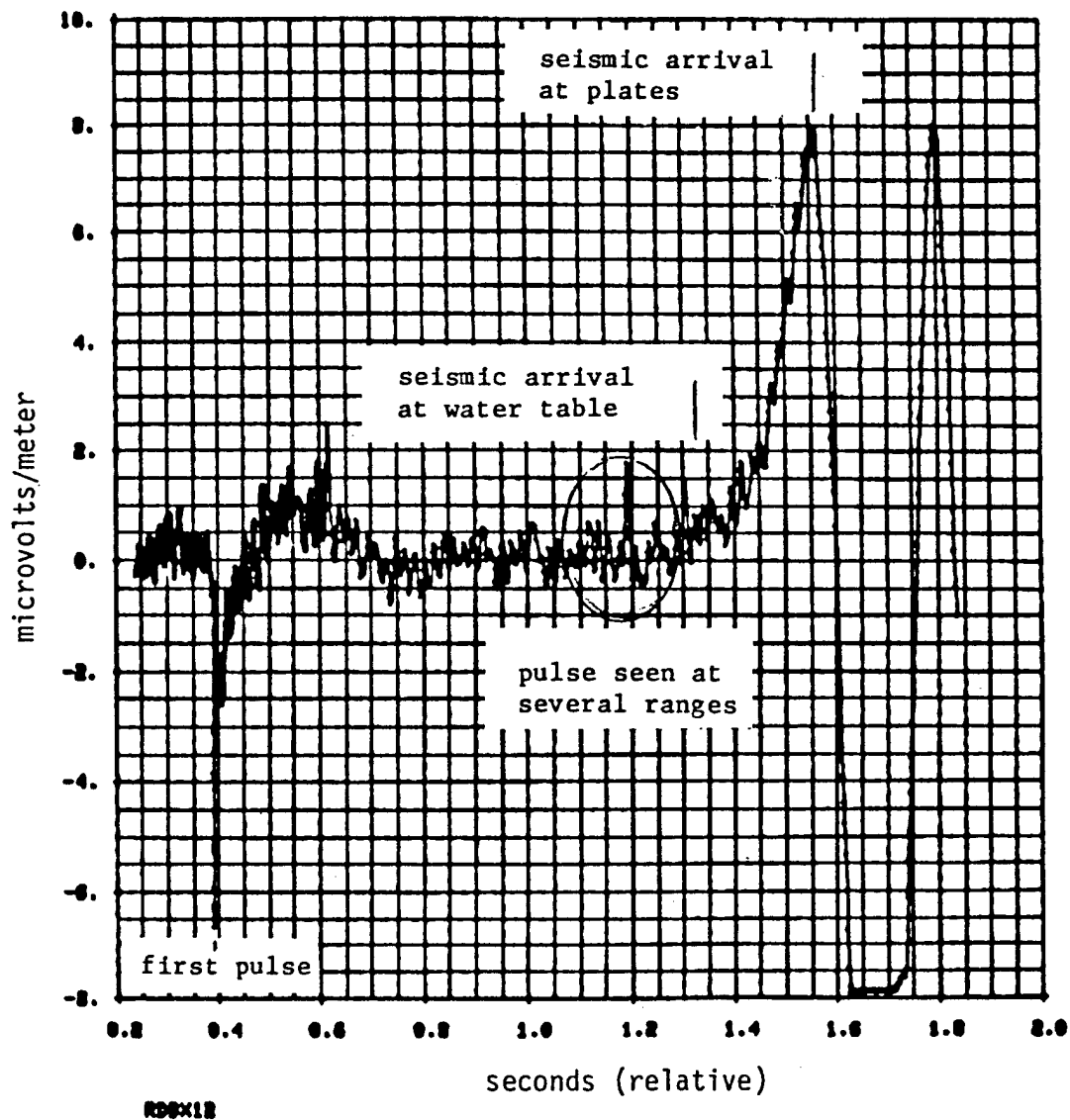


Fig. F-6. Draughts Event EMP--Buried plates near U9cn.
 Distance: 4.7 km
 Azimuth from GZ: N4°E
 Plate Separation: 300 m
 Plate Orientation: N30E

APPENDIX G
FITZHUGH'S LOWBALL DATA

A number of earth potential measurements were made by R. Fitzhugh on event Lowball. The locations of some of his buried plates are shown on the map of Fig. G-1; ranges to the plates from ground zero, from his trailer park, and from each other in some cases are given in Table G-I. Measurements were made of the plate potential compared with the reference potential at the trailer park; and, in some cases, measurements were also made of the potential difference between selected plates. A selection of some of those data is depicted in Figs. G-2--G-6; the upper waveform in each figure is on a 0.03 s time base; the lower, a 6-s time base. Figures G-7 and G-8 are on 3- and 30-ms time bases; Fig. G-9 is on a 30-ms time base. The figure number below each record is Fitzhugh's designation from his memo.

TABLE G-I
DISTANCE TO POTENTIAL PLATES

		<u>Distance (km)</u>
GM	- GM-1	1.37
	GM-4	1.04
	GM-6	1.48
	GM-8	2.01
	GM-9	2.20
Trailer park -	GM-1	0.30
	GM-4	0.57
	GM-6	1.20
	GM-8	1.02
	GM-9	1.40
	GZ	1.08
GM-6	- GM-8	2.05
GM-4	- GM-9	1.94

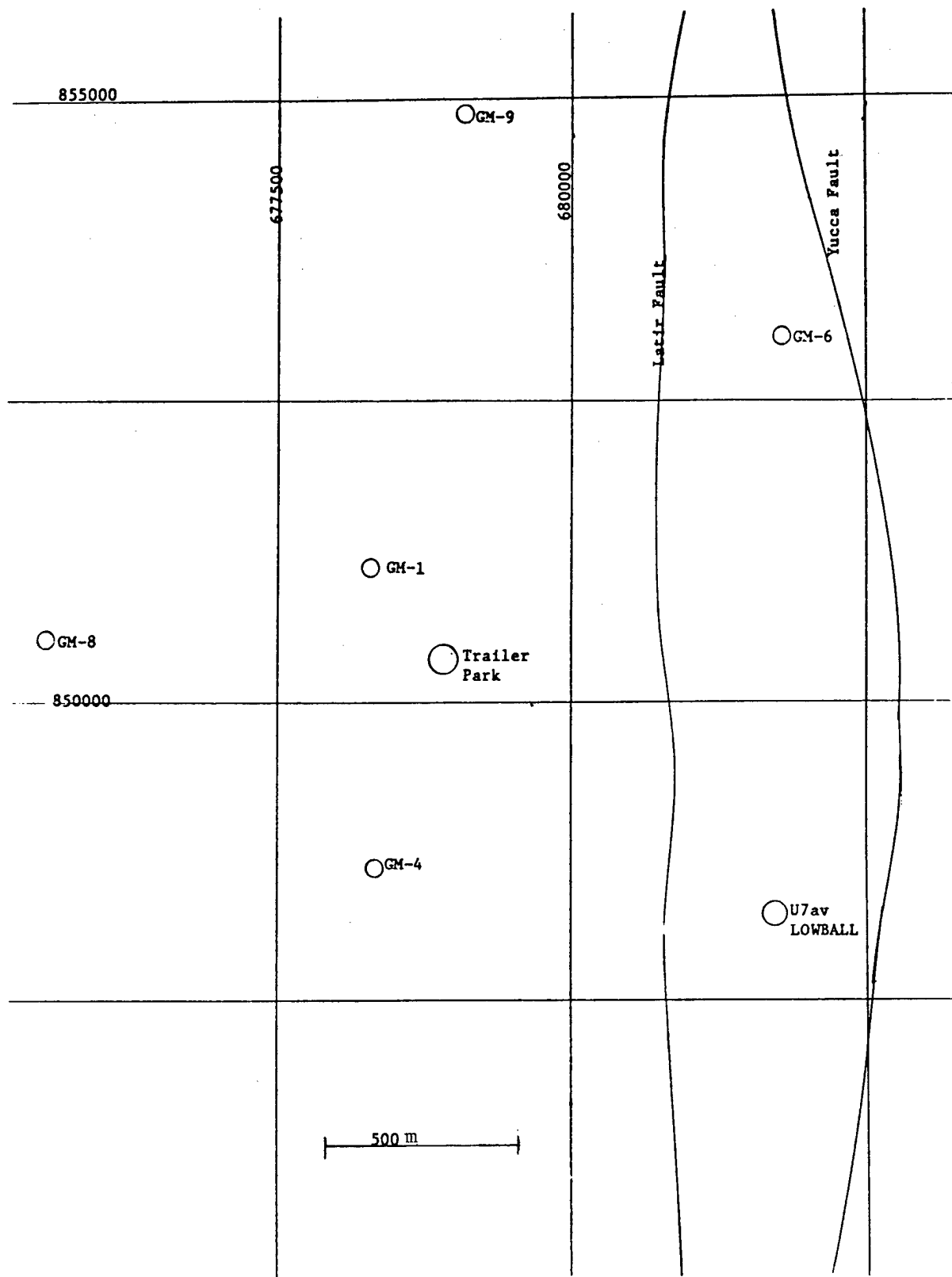


Fig. G-1. Locations of ground potential plates used on Lowball.

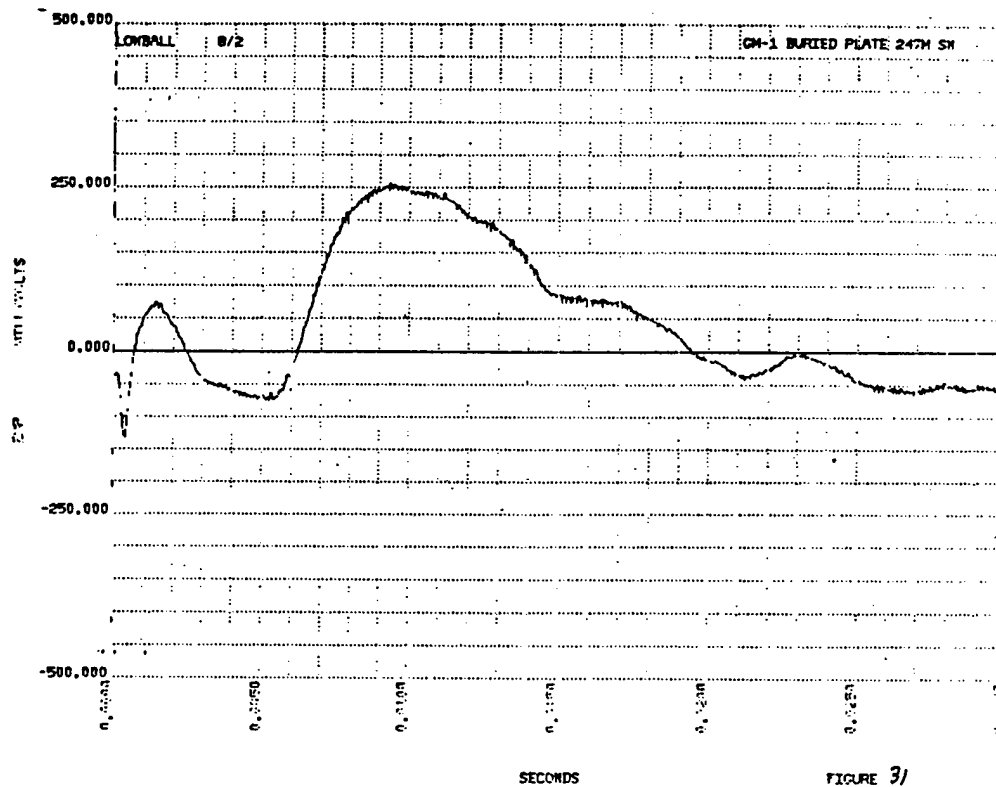


FIGURE 3/

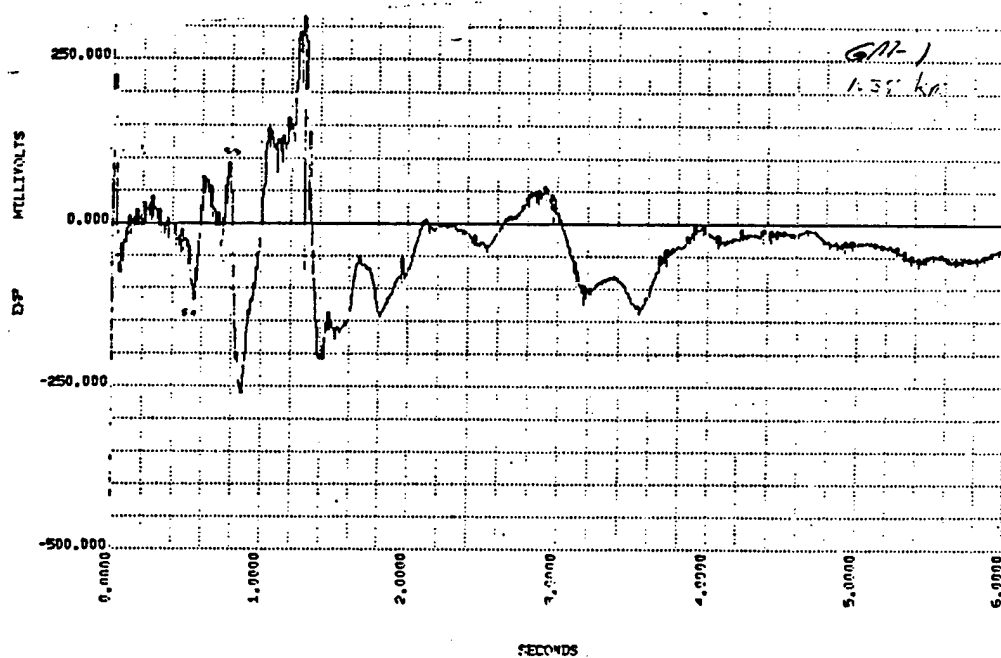


Fig. G-2. Data from GM-1 plates--1.37 km, NW.

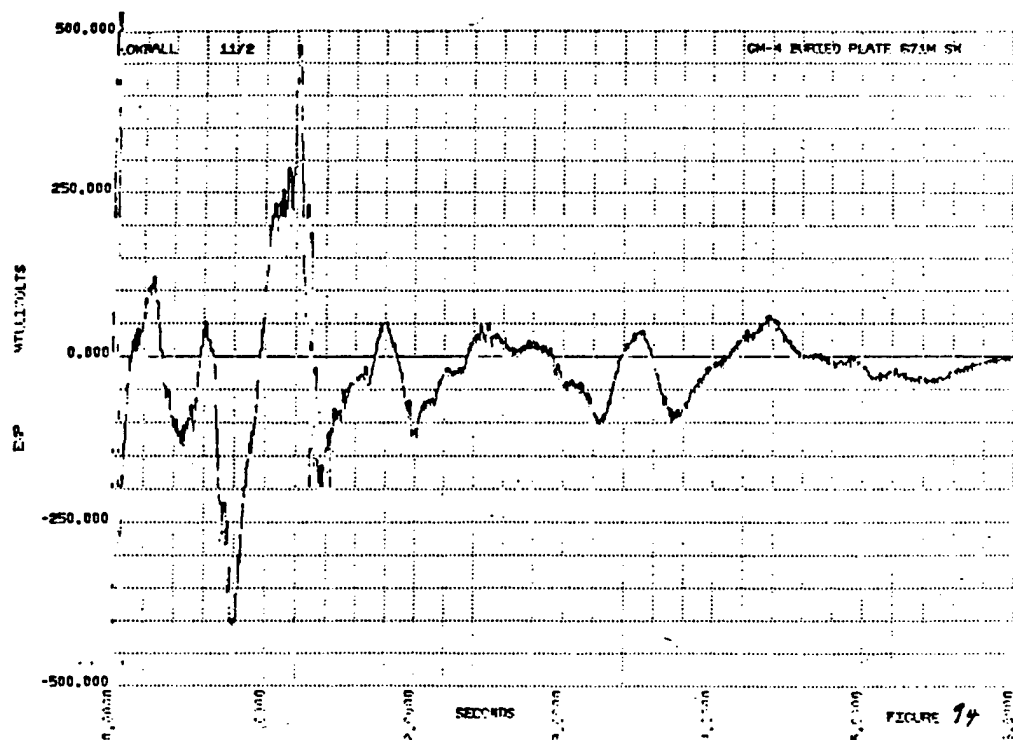
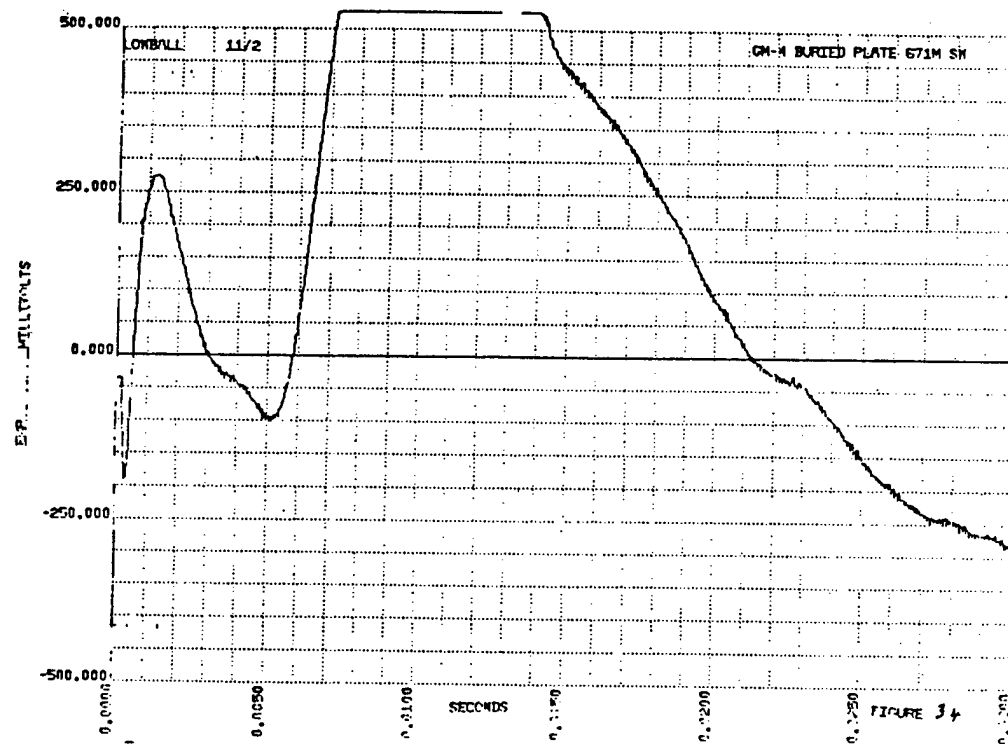


Fig. G-3. Data from GM-4 plates--1.04 km, W.

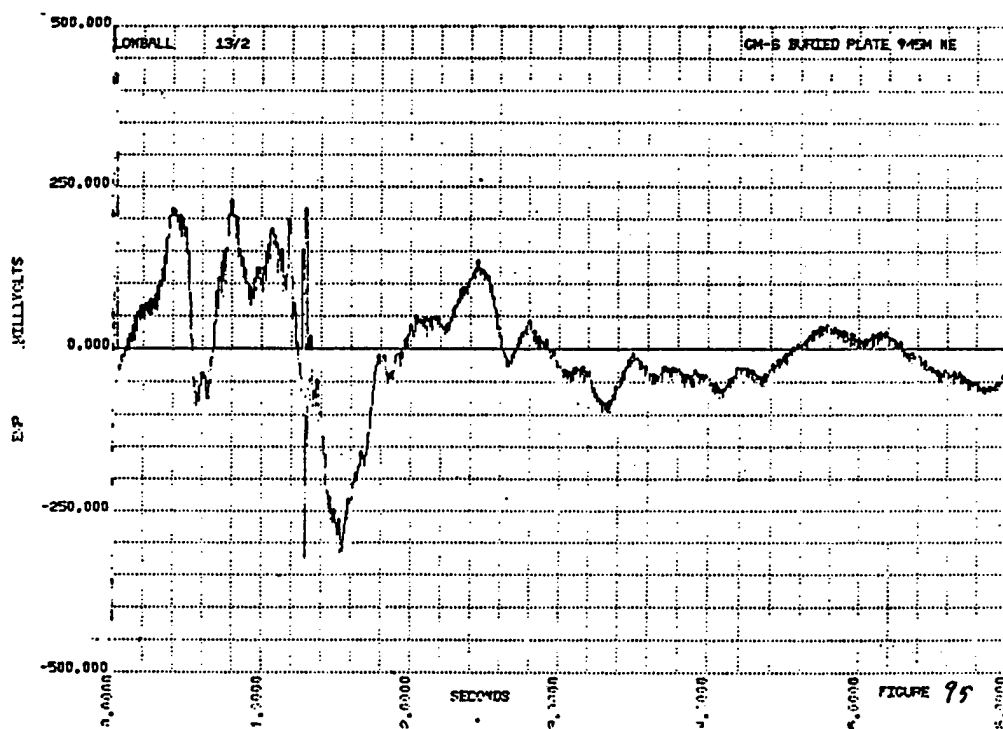
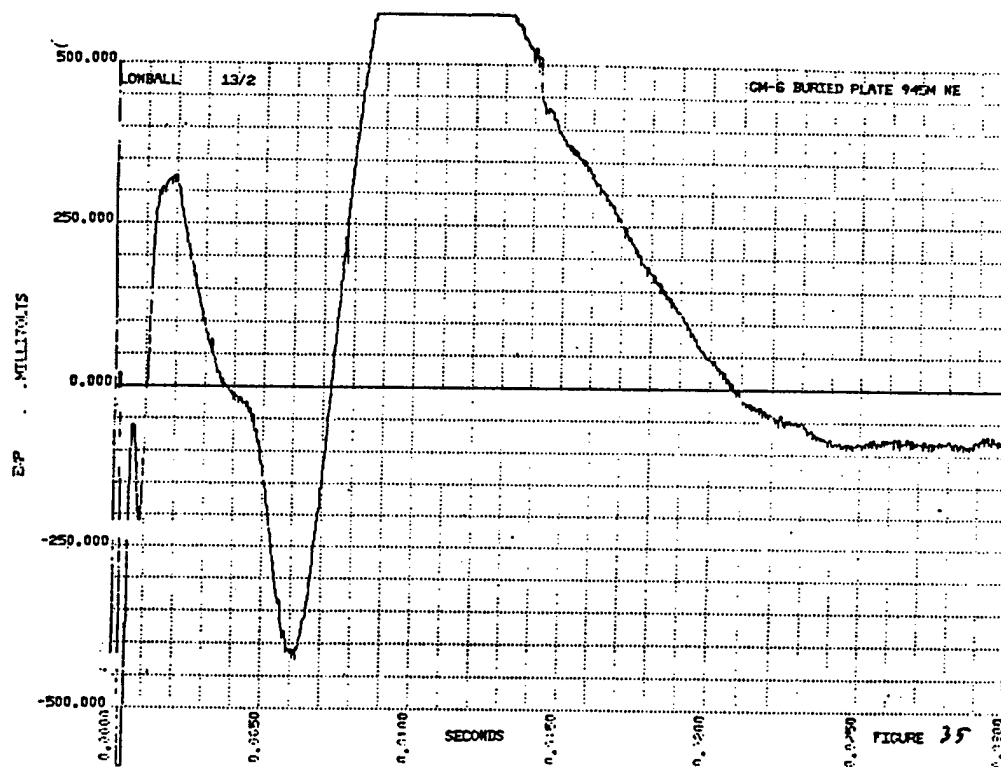


Fig. G-4. Data from GM-6 plates--1.48 km, N.

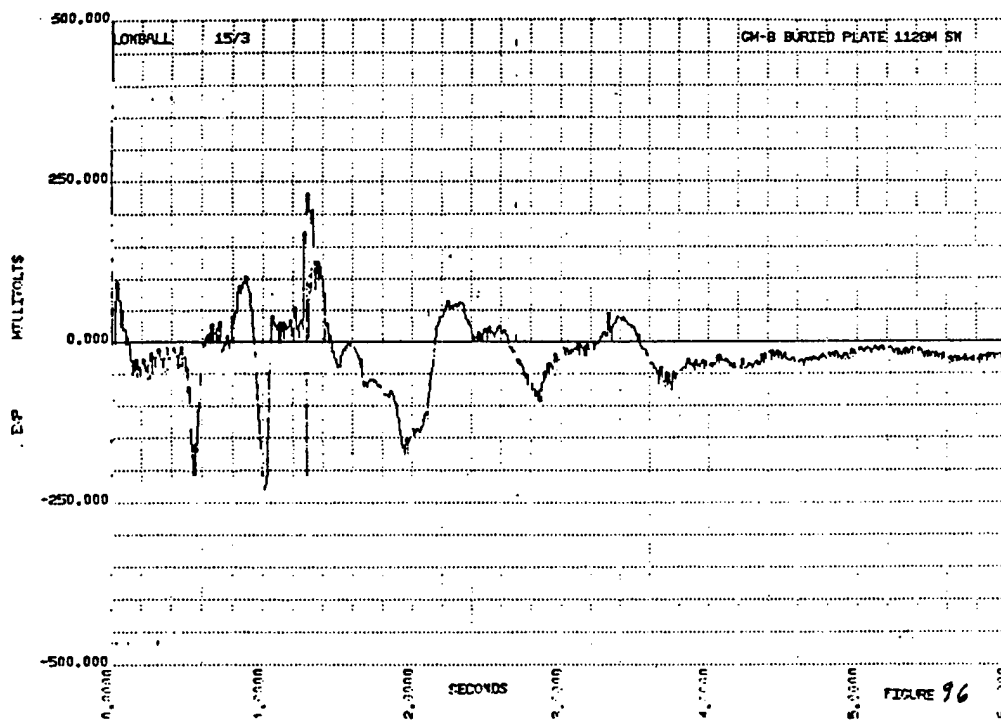
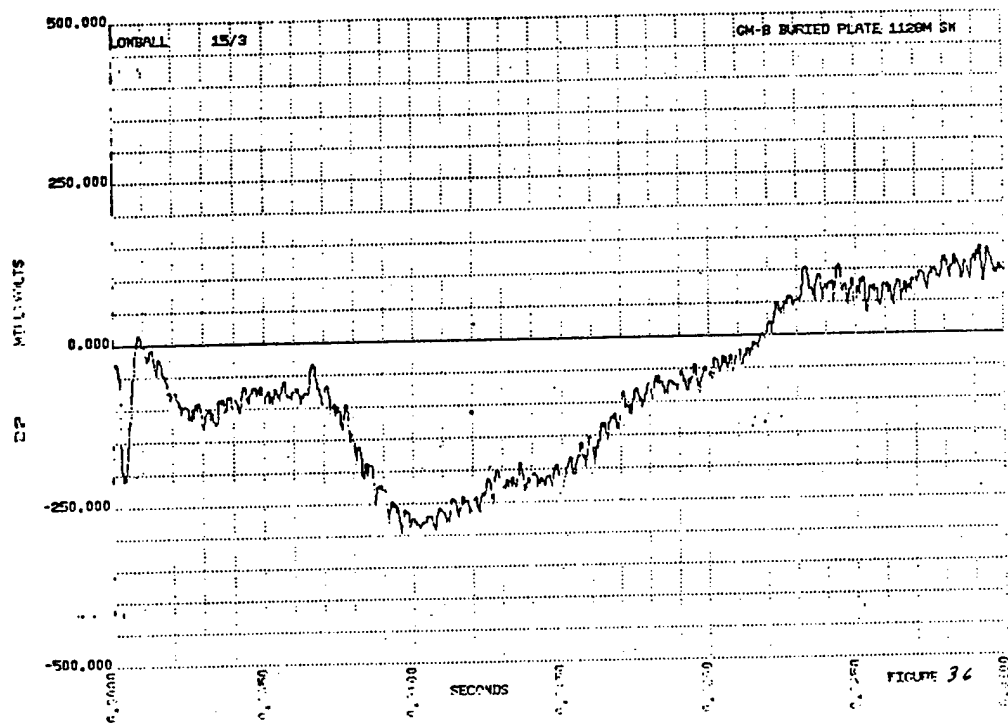


Fig. G-5. Data from GM-8 plates--2.01 km, WNW.

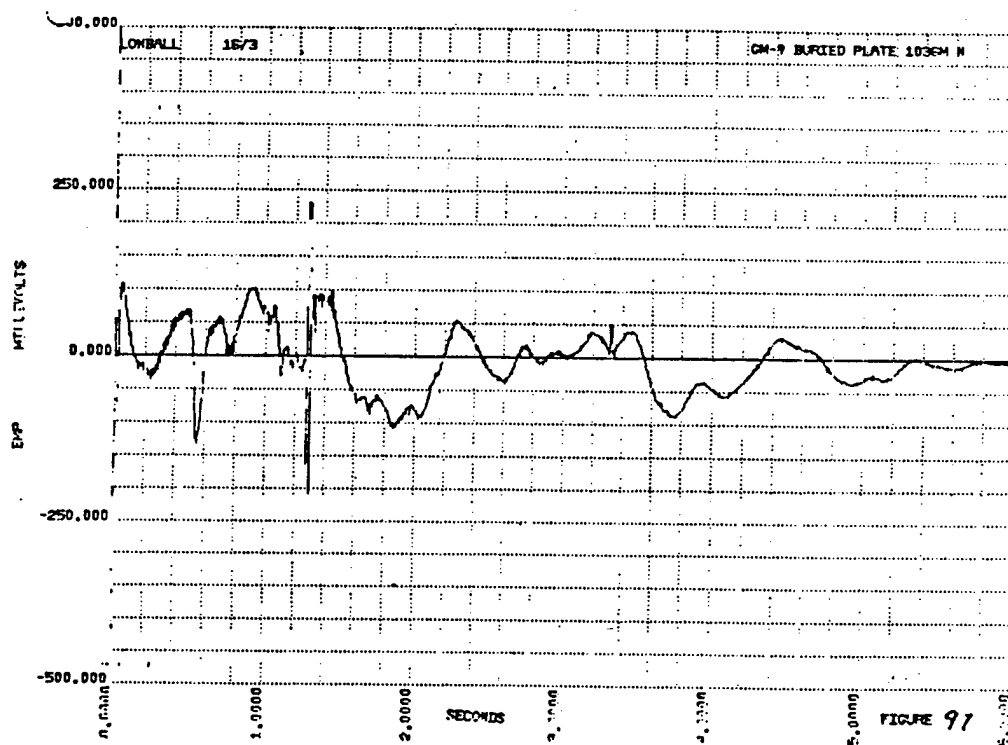
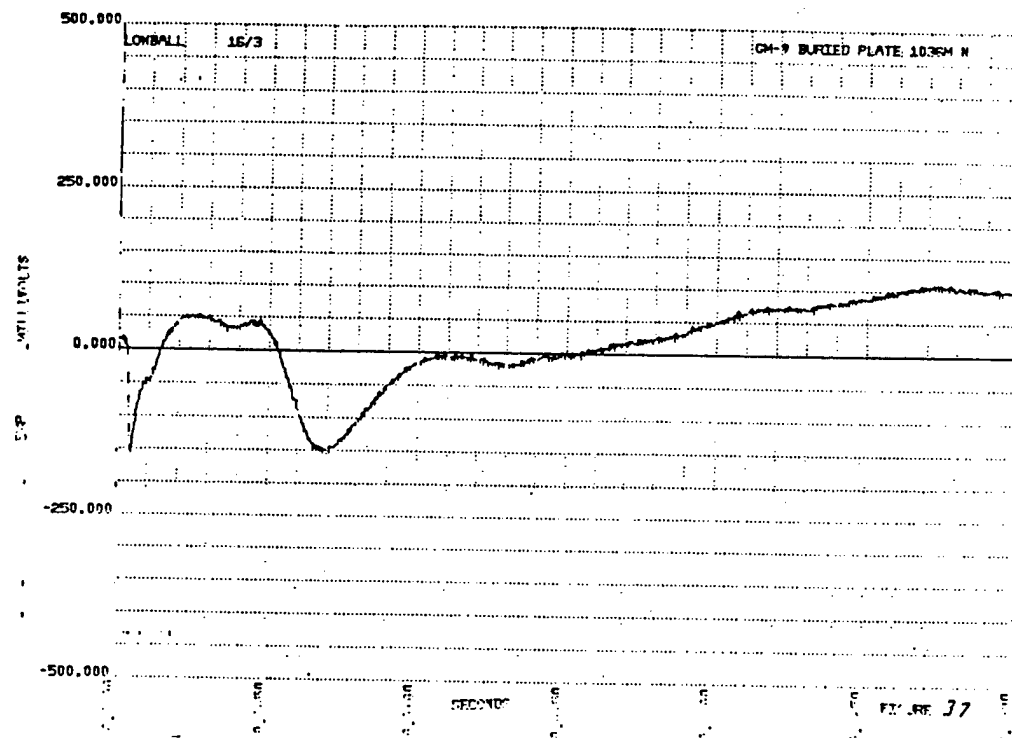


Fig. G-6. Data from GM-9 plates--2.20 km, NNW.

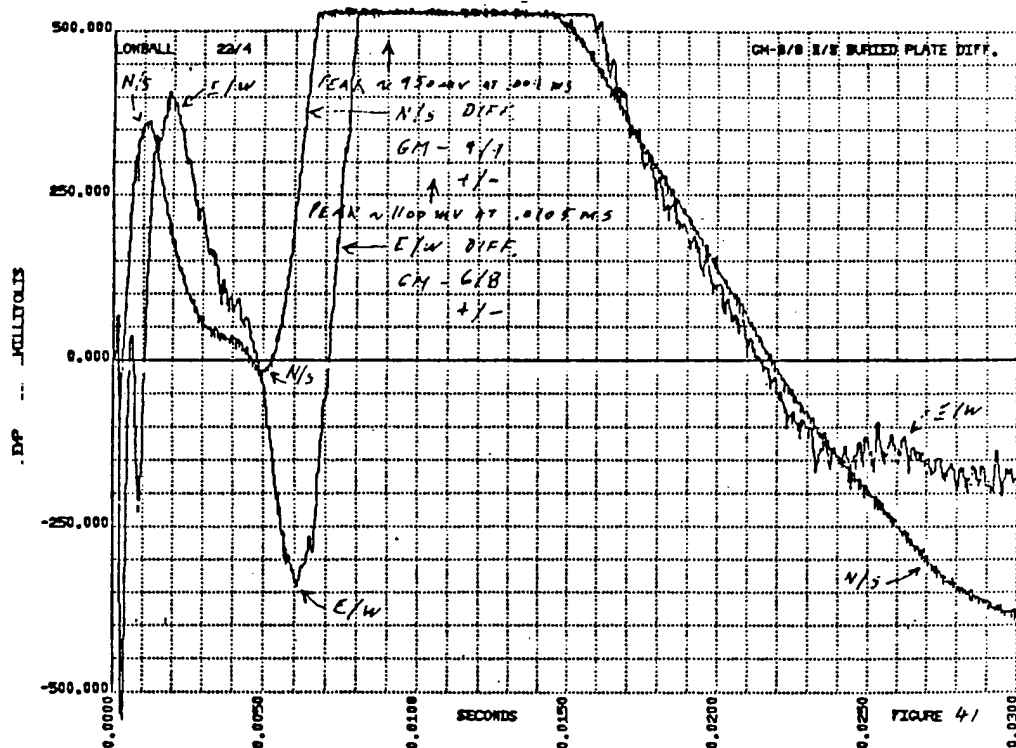
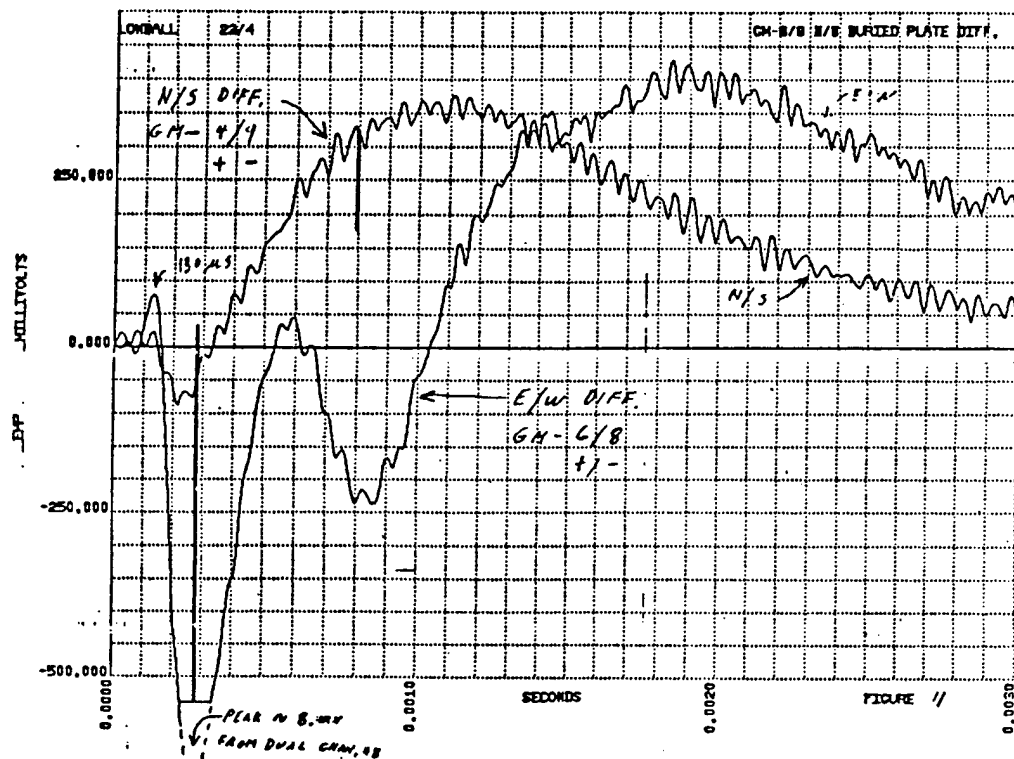


Fig. G-7. Differential between GM-6 and GM-8 plates E/W, 2.05-km separation--3- and 30-ms time bases.

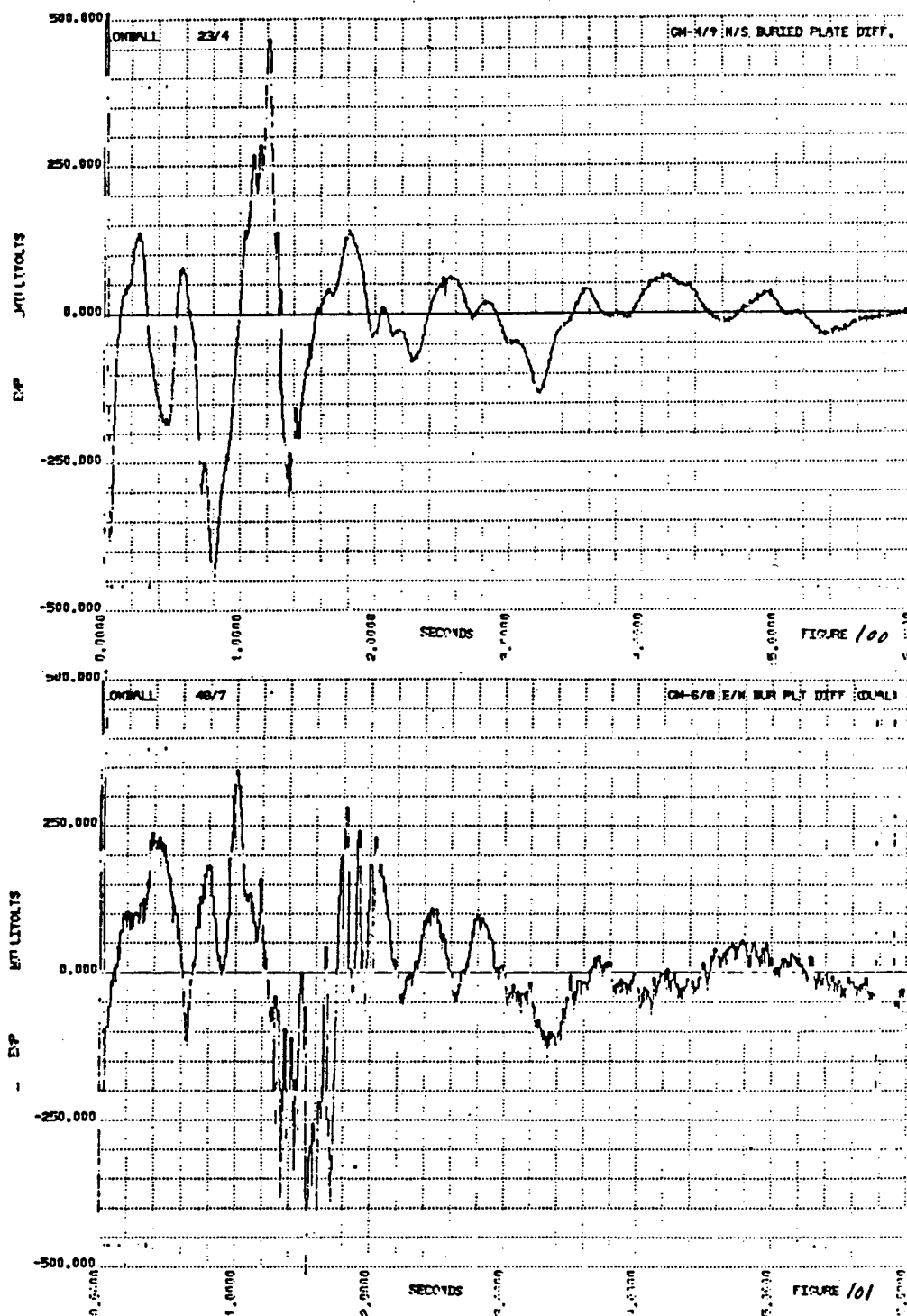


Fig. G-8. Differential between GM-6 and GM-8 (upper) and GM-4 and GM-9 (lower)--6-s time bases.

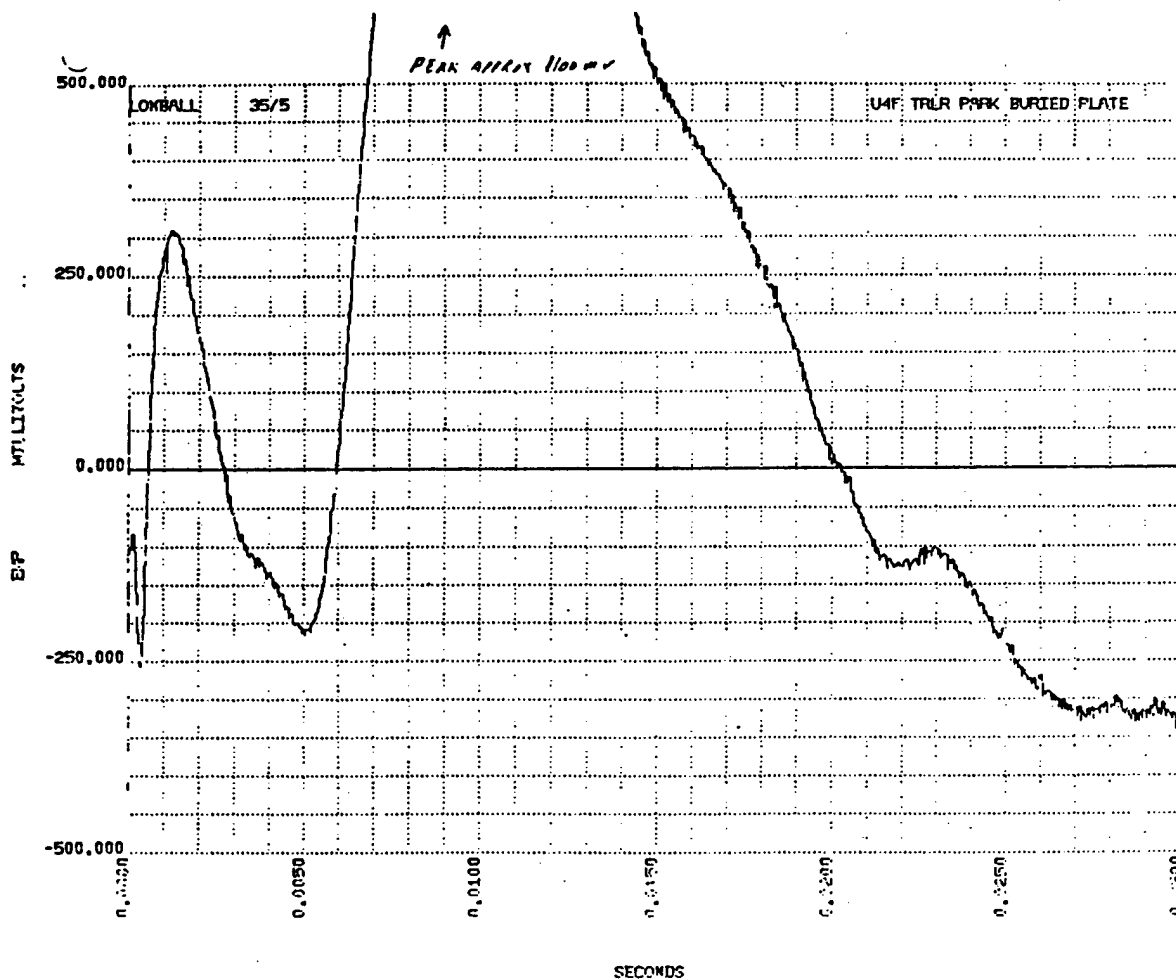


Fig. G-9. Potential on trailer park ground--30-ms time bases.

It is not clear if the data are readily interpreted as the trailer park ground to reference ground showed a large signal as well (Fig. G-9). At least some parts of the data have significance. A summary of information relating to Lowball and to two of the stations is given in Table G-II. The initial pulse may be due to a signal propagated to the surface, thence along the surface to the plate. The pulse at about 5 ms may be due to the signal from diffusion through the medium to the trailer park; that time is about 5 ms and it shows on all records as it is the reference level. As the GM-1 plate is near the trailer park, with a diffusion time of 7 ms, it probably has a mixed signal of reduced amplitude. The signals on the shorter time scale records thus appear to be diffusion signals. They could be due either to the magnetic bubble or to the electroseismic effect. The azimuthal dependence ought to delineate which, but it does not. The bubble signal ought to be less affected by the inhomogeneities of the medium and exhibit a dipole azimuthal dependence. As it does not, it is discounted as a plausible mechanism. The electroseismic signal ought to be radial, but inhomogeneities could readily introduce transverse components.

The longer time base records clearly show signals before seismic arrival at the plates. One of these signals seems to be simultaneous with the time of shock arrival at the surface (0.3 s). It appears at a time corresponding to propagation to the Paleozoics, thence back to the depth of the static water level (0.5 s). Plate GM-1 displays a signal at about 0.7 s, which corresponds both to seismic arrival at the trailer park and to the time to the P_2 layer, through the layer, thence up to the SWL. This time is 0.86 s for plate GM-9, which does show a signal near this time. This postulate seems to provide an explanation for the signals that are recorded at a location before seismic arrival itself. The best evidence, however, is Homuth's data (Appendix F), also from Lowball.

TABLE G-II

LOWBALL SUMMARY

Depth of burial	564 m
Medium	Saturated tuff
Static water level	500 m
Depth to Paleozoics	900 m
Average seismic velocity WP to surface	1.8 km/s
Seismic velocity at WP	2.65 km/s
Seismic velocity in P_z	5-6 km/s
Cavity radius	65 m
Average conductivity	0.01 S/m

Diffusion times: $\tau = \mu \sigma l^2 / 4$

WP to surface 1.1 ms

WP to GM-1 7 ms

WP to GM-9 16 ms

WP to trailer park 5 ms

Seismic arrival times:

GZ 0.33 s

GM-1 0.83 s

GM-9 1.26 s

Trailer park 0.68 s

WP to P_z + P_z to plate sub-point + P_z to SWL

GM-1 0.7 s

GM-9 0.86 s

WP to P_z + P_z to SWL: 0.49 s

Slapdown time 1.62 s

REFERENCES

1. J. Malik, "Electromagnetic Fields and Ground Currents from Underground Nuclear Explosions," Los Alamos Scientific Laboratory memorandum J-D0 (March 1964).
2. C. J. Zablocki, "Electrical Transients Observed during Underground Nuclear Explosions," J. Geophys. Res. 71, 3523-3542 (1966).
3. R. Fitzugh, "Earth Current Measurements," Los Alamos Scientific Laboratory memorandum J-8-76-36 (February 9, 1976) and J-8-76-58 (March 22, 1976).
4. A. N. Sommerfeld, "The Propagation of Waves in Wireless Telegraphy," Ann. Phys., Series 4, 28, 665 (1909); 81, 1135 (1926); and in Partial Differential Equations (Academic Press, New York 1949).
5. A. Banos, Dipole Radiation in the Presence of a Conducting Half-Space (Pergamon Press, Oxford, 1966).
6. R. K. Moore and W. E. Blair, "Dipole Radiation in a Conducting Half-Space," J. Research NBS 65D, 547-563 (1961).
7. J. R. Wait, "Propagation of Electromagnetic Pulses in a Homogeneous Conducting Earth," Appl. Sci. Res. 8B, 213-253 (1960).
8. L. W. Miller, "The Electromagnetic Pulse from an Underground Nuclear Explosion," Los Alamos Scientific Laboratory report LA-5056 (January 1973).
9. C. J. Zablocki and G. V. Keller, "Some Observations of the Seismic-Electric Effect," D-296-D-299 USGS Denver Geological Survey research paper 395, (1961).
10. S. T. Martner and R. N. Sparks, "The Electrostatic Effect," Geophys. 24, 297-308 (1959).
11. J. Frenkel, "On the Theory of Seismic and Seismoelectric Phenomena in a Moist Soil," J. Phys. 8, 230-241 (1941).

OTHER USEFUL SOURCES

- J. R. Wait, "The Electromagnetic Fields of a Horizontal Dipole in the Presence of a Conducting Half-Space," Can. J. Phys. 39, 1017-1028 (1961)--HED.
- J. R. Wait and L. L. Campbell, "The Fields of an Oscillating Magnetic Dipole Immersed in a Semi-Infinite Conducting Medium," J. Geophys. Res. 58, 167-177 (1953)--HMD.
- J. R. Wait, "The Magnetic Dipole over the Horizontally Stratified Earth," Can. J. Phys. 29, 577-592, (1951).
- J. R. Wait and L. L. Campbell, "The Fields of an Electric Dipole in a Semi-Infinite Conducting Medium," J. Geophys. Res. 58, 21-28 (1953)--VED.

**DEFENSE TECHNICAL INFORMATION CENTER
REQUEST FOR SCIENTIFIC AND TECHNICAL REPORTS**

Title "Electrical Magnetic Signals from under ground nuclear Explosions"

1. Report Availability (Please check one box)

- ☒ This report is available. Complete sections 2a - 2f.
☐ This report is not available. Complete section 3.

**2a. Number of
Copies Forwarded**

1

2b. Forwarding Date

6/31/2000

2c. Distribution Statement (Please check ONE box)

DoD Directive 5230.24, "Distribution Statements on Technical Documents," 18 Mar 87, contains seven distribution statements, as described briefly below. Technical documents **MUST** be assigned a distribution statement.

- ☒ DISTRIBUTION STATEMENT A: Approved for public release. Distribution is unlimited.
- ☐ DISTRIBUTION STATEMENT B: Distribution authorized to U.S. Government Agencies only.
- ☐ DISTRIBUTION STATEMENT C: Distribution authorized to U.S. Government Agencies and their contractors.
- ☐ DISTRIBUTION STATEMENT D: Distribution authorized to U.S. Department of Defense (DoD) and U.S. DoD contractors only.
- ☐ DISTRIBUTION STATEMENT E: Distribution authorized to U.S. Department of Defense (DoD) components only.
- ☐ DISTRIBUTION STATEMENT F: Further dissemination only as directed by the controlling DoD office indicated below or by higher authority.
- ☐ DISTRIBUTION STATEMENT X: Distribution authorized to U.S. Government agencies and private individuals or enterprises eligible to obtain export-controlled technical data in accordance with DoD Directive 5230.25, Withholding of Unclassified Technical Data from Public Disclosure, 6 Nov 84.

2d. Reason For the Above Distribution Statement (in accordance with DoD Directive 5230.24)

2e. Controlling Office

Report Library
Jack Carter as Names Noted

**2f. Date of Distribution Statement
Determination**

10-1985
Laboratory

3. This report is NOT forwarded for the following reasons. (Please check appropriate box)

- ☐ It was previously forwarded to DTIC on (date) and the AD number is
- ☐ It will be published at a later date. Enter approximate date if known.
- ☐ In accordance with the provisions of DoD Directive 3200.12, the requested document is not supplied because:
.....
.....
.....

Print or Type Name

Jack Carter

Signature

Jack Carter

Telephone

505-667-4446

(For DTIC Use Only)

AQ Number *U00-08-1889*